MEASUREMENT OF CUTTING TEMPERATURES IN SYNTHETIC DIAMOND CUTTERS DURING ROCK CUTTING

by

P. MADHUSUDHAN

B.S.(Honors), University of Madras, India, 1981

A MASTER'S THESIS

submitted in partial fulfillment of the
requirements for the degree

MASTER OF SCIENCE

Department of Industrial Engineering

KANSAS STATE UNIVERSITY
MANHATTAN, KANSAS

1988

Approved by:

Doris Grosh
Major Professor

F. C. Appl
Major Professor

LL
0968
.T4
IE
1988
M35
C.2

A11208 231494

CONTENTS

LIST OF FIGURES..... ii

1.0 INTRODUCTION..... 1

2.0 METHODS OF TEMPERATURE MEASUREMENT..... 17
2.1 Temperature: some basic ideas..... 17
2.2 Thermocouple temperature measurements..... 18
2.3 Laws of Thermoelectric Circuits..... 23
2.4 Elementary Thermoelectric Circuit..... 26
2.5 Thermocouple Reference Tables..... 26
2.6 Introduction to Infrared Radiation..... 29
2.7 Infrared Detectors..... 30
2.8 Types of Detectors..... 33
2.9 Optics..... 35
2.10 Instrumentation..... 36

3.0 CUTTING TEMPERATURE MEASUREMENTS..... 44
3.1 Methods of tool temperature measurement... 44
3.2 Literature survey..... 47

4.0 EXPERIMENTAL ARRANGEMENT..... 62
4.1 Metal Cutting..... 62
4.2 Rock Cutting..... 63

5.0 RESULTS AND DISCUSSION..... 69
5.1 Experiment #1 and #2 on Metal Cutting..... 69
5.2 Rock Cutting Experiments..... 71

6.0 CONCLUSIONS AND RECOMMENDATIONS..... 78

REFERENCES..... 81

APPENDIX A (Conversion Tables for K type thermocouples) 83

APPENDIX B (Experimental Data)..... 91

APPENDIX C (Photographs)..... 94

ACKNOWLEDGEMENTS..... 96

LIST OF FIGURES

Figure		Page
1.	A P.D.C. Drill bit	3
2.	A P.D.C. Drill bit	3
3.	A P.D.C. cutter	4
4.	A P.D.C. drill bit	4
5.	Experimental results of Lee and Hibbs	10
6.	Experimental results of Lee and Hibbs	11
7.	Temperature contours in the tool - Prakash	13
8.	Temperature Distribution along the Rake Face	14
9.	Temperature Distribution along the bottom face	15
10.	Ice bath circuit	21
11.	The emf is unaffected by the third material C	25
12.	Emfs are additive for materials	25
13.	Emfs are additive for temperature intervals	25
14.	Basic thermocouple circuit using K type	27
15.	Temperature versus emf curves	28
16.	Block diagram of infrared radiometer	39
17.	Radiometer for temperature measurement	39
18.	Proposed setup for infrared measurement	42
19.	Embedded thermocouple technique	46
20.	Method of determining temperatures	50
21.	Thermoelectric measurement of grinding temperature	52
22.	Temperature and heat flow measuring equipment	52
23.	Location of miniature thermocouple	56
24.	Pyrometer system used by Ueda et al	56

LIST OF FIGURES - Continued

Figure		Page
25.	Fundamental measuring system with optic fiber.....	56
26.	Experimental arrangement (Ueda et al).....	60
27.	Experimental arranngement (Ueda et al).....	60
28.	Tungsten carbide tool for Experiment #1.....	64
29.	Tungsten carbide tool for Experiment #2.....	64
30.	Tool holder and thermocouple assembly.....	65
31.	Tool holder and thermocouple assembly.....	65
32.	Tool holder used for rock cutting experiment.....	66
33.	Temperature plots for metal cutting experiments..	70
34.	Temperature plot for rock cutting Experiment #3...	72
35.	Temperature Vs Distance plot for Experiment #4....	74
36.	Temperature Vs Distance plot for Experiment #5....	76

1.0 INTRODUCTION

The introduction of synthetic polycrystalline diamond compact (PDC) cutters for use as cutters on oil well drill bits by General Electric in 1973 was a significant advance in drilling technology [1]. The development of these PDC cutters was largely based on trial and error experimental research and only a minimal amount of basic research. To realize the full potential of this type of cutter there is an urgent need to develop an improved theoretical model of the cutting mechanics, heat transfer and wear for these cutters. To verify and/or determine inaccuracies in the already developed and future theories, experiments have to be developed.

Until the early 70's, there were basically two kinds of drill bits; three cone toothed roller bits (rock bits) and diamond (natural) bits. The rock bits were used for soft and medium to medium-hard rocks, and diamond bits were used for medium-hard to hard rocks. It was commonly known that bladed bits, known as drag bits, could drill some soft to medium formations at higher rates of penetration than rock bits. But these bits typically were rough running due to the small number of cutters (3 or 4) and hence were seldom used. Large fluctuations in torque increased the danger of twist-off sufficiently to outweigh the potential increase in rate of penetration. In fact, however, the drag type cutter has the potential to be one

of the most effective means of mechanical cutting. To achieve this it is desired to attain a strong cutter that, during use, maintains a flat cutting face, has a rake angle of approximately zero degrees, and has a sharp cutting edge. It is further desired that, as the cutter wears, the area of the wear flat remain as small as possible. This method of cutting is used quite successfully for machining ductile metals. If this could be achieved for cutting rock, drill bits could be developed that would have high rates of penetration with relatively low bit weight. It was recognized in the late 50's that one approach to this was to devise a cutter consisting of two different materials. A relatively thin layer of hard, abrasive resistant material should be used for the face of the cutter and this should be backed by a thicker layer of strong, but easily abraded backup material. Considerable effort was made to develop such a workable combination consisting of tungsten carbide for the facing and steel for the backup. The work, however, was largely unsuccessful; partly because the materials were not adequate and partly because only bits with a few large blades were tried.

This basic concept of cutters which consist of different materials was reborn in 1973 when General Electric Company began experiments with a new type of drag bit which utilized the newly developed synthetic

Figure 1: A P.D.C. Drill bit

Figure 2: A P.D.C. Drill bit

Figure 3: A P.D.C. cutter

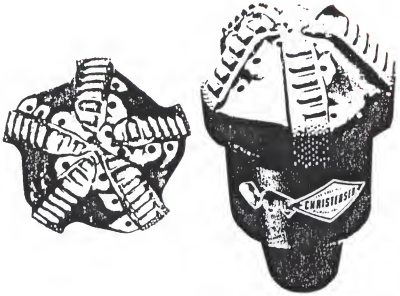

Figure 4: A P.D.C. drill bit

polycrystalline diamond compacts (PDC) as the cutting elements. A PDC cutter is shown in Figure 3. Examples of PDC drill bits are shown in Figures 1, 2 and 4. These are circular tungsten carbide discs with a layer of synthetic diamond bonded on one face. These discs are mounted edgewise on the bit face to serve as cutting elements. These discs are approximately 1/2 inch in diameter which allows many discs to be mounted on the bit face. Used in this fashion these discs act as drag type cutters and, because of the relatively large number, the bits run smoother than the former blade type drag bits. There is still a tendency to run rougher than rock bits so it is important to place the cutters in a geometric pattern that minimizes torque unbalance. This is an important aspect of the design of these bits.

Soon after the introduction of PDC bits, a major problem was encountered. To prevent thermal damage to the diamond, a low temperature braze material was used to attach the PDC discs. This material was not strong enough, and many cutters were lost during bit operation. Considerable effort was devoted to the solution of this problem and techniques were developed which virtually eliminated the problem. This spurred further interest in this style of bit and led to rapid development and widespread application of PDC bits. Until the middle of this decade, work was done largely by trial and error,

with only a minimal amount of basic research on the cutting action of PDC cutters. Research has been largely devoted to experimental and theoretical work related to the mechanical aspects of cutting. It has been recognized, however, that the synthetic diamond compact material which is currently used deteriorates rapidly (loses strength and abrasion resistance) at temperatures exceeding 700-750 deg. C [2]. This is thought to be one of the main reasons that it has not been possible to successfully drill the harder formations with PDC bits. Potentially, however, drag type cutting is a very effective method of mechanical cutting and there is no apparent reason why this basic type of cutter cannot be used to drill hard rocks, if the cutters are properly designed and utilized on the drill bit and if the drilling operation is properly controlled.

What is needed to continue the improvement of PDC bits is to experimentally verify developed theoretical models for the heat transfer and temperature distributions in the rock and cutters near the cutting tips of the cutters. Prakash [1] developed a combined theoretical model of cutting, heat transfer and wear rate for PDC cutters. A need for designing and conducting experimental cutting tests was felt to be necessary for verification of this model. These tests which include measurement of wear rate and temperature will indicate

deficiencies, if any, in the theory and thus enable further improvements to be made.

The significance of this work is that when an adequate model is achieved, it will be possible to use it to develop improved bit designs, to establish improved operating parameters (RPM, Bit Weight, etc.) and ultimately to dynamically control drilling by means of MWD (Measurement While Drilling). It is expected that significant design improvements can be achieved, because, not only will it be possible to design bits to maintain diamond temperatures below the critical value, but also the effects of other cutter design variables can be evaluated and included in the design.

One of the many factors that make oil well drilling difficult and complex is that the drilling action takes place at the bottom of the borehole, which may be thousands of feet deep, and thus it is not possible to observe the behavior of the bit during drilling. Furthermore, until quite recently, no downhole measurements of bit performance were made because there was no practical way to transmit data from the bit to the surface. MWD systems are now being developed by the industry and promise to provide measurement and transmission of bit performance data to the surface. This will afford the opportunity to implement more rational methods of controlling the drilling process.

A feedback control system for drilling can be developed by using MWD to transmit real time drilling and formation data to the surface, and by using an on site computer to control the drilling operation. The computer will utilize the drilling model to interpret the data transmitted by MWD to make the required control decisions.

Most important of all, however, is that the improvements in drilling performance that are achieved will result in reductions in the cost of drilling, which are so vitally needed to maintain an adequate supply of energy at a reasonable price.

Lee and Hibbs [2] are credited with the only known experimental work in which strength vs. temperature data and rock cutting and wear data were measured for the same diamond material. A single PDC cutter was used in this experiment. Rock cutting tests were carried out turning the cylindrical surface of a cored specimen of Jackfork Sandstone on a conventional lathe. Jackfork Sandstone, obtained from a quarry in Arkansas, is a strong (uniaxial, unconfined compressive strength ~ 30000-35000 psi) well bonded, highly abrasive rock with a high quartzite content and has been used extensively for accelerated wear studies of diamond materials. The polycrystalline sintered diamond compact tools used were 0.325 in. diameter with ~0.025 in. diamond layer. Two tool holder geometries were used: (1) -5 deg. back rake, -5 deg.

side rake and (2) -15 deg. back rake, 0 deg. side rake. The former was used with a feed rate of 0.005 in. per revolution and the latter with a feed rate of 0.020 in. per revolution. A depth-of-cut of 0.020 in. was used in all cases.

The effect of cutting speed on wear rate for a polycrystalline sintered diamond compact tool as obtained by Lee and Hibbs is shown in Figure 5. The volumetric wear per unit distance of tool travel was strongly influenced by speed (and thus, by temperature). Tests with cutting velocities up to 650 fpm were conducted. In contrast with earlier tests (wear and breakage mechanisms essentially mechanical at cutting speeds below 350 fpm), they found that with the extended range of velocity, an abrupt increase in the wear rate of the diamond at 410 fpm took place. It was suspected that this was related to the effects of increased cutter temperature, so a series of microhardness tests vs. temperature were made for the same type of synthetic diamond (Figure 6). This indicated that the microhardness decreased abruptly in the temperature range of 700-750 deg. C. This suggests that the abrupt increase in wear rate in the cutting tests is due to decreased mechanical strength, resulting from the increased cutter temperature. Unfortunately, no measurements of cutter temperature were made, so a direct correlation with hardness was not possible. Lee and

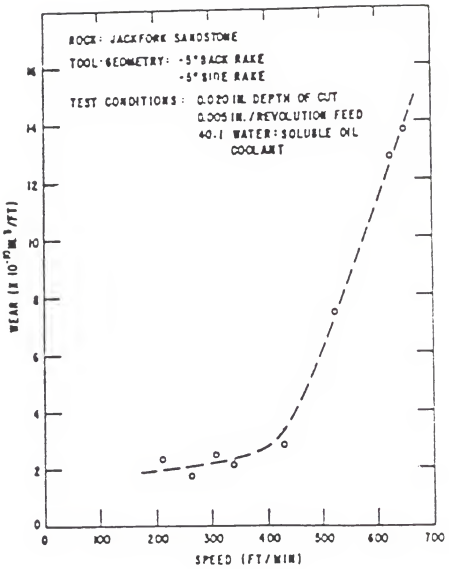

Figure 5: Experimental results of Lee and Hibbs Velocity vs. Wear

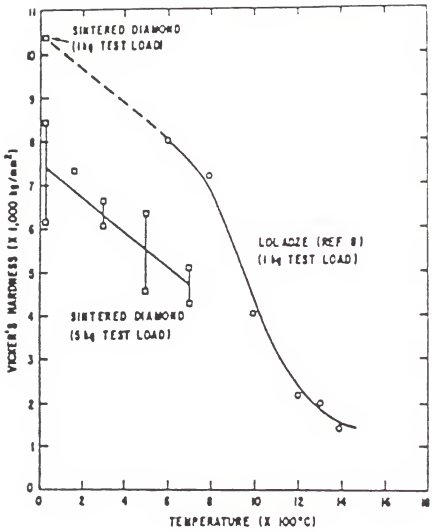

Figure 6: Experimental results of Lee and Hibbs
Temperature vs. Hardness

Hibbs' work serves as a cross verification for additional experiments to be designed and conducted for refinement of the model.

Finite element method was applied by Prakash [1] to develop a theoretical model for the heat transfer and temperature distribution for PDC cutters. His maximum temperature prediction of 713.33 deg. for a cutter velocity of 430 fpm (Figures 7-9) correlated the two sets of data from the Lee and Hibbs experiments. This was a significant result since it confirmed the validity and accuracy of the thermal model. Prakash recommended conducting additional experiments to obtain additional verification and refinement. This model if found adequate, can be used as a basis for designing the instrumentation for temperature measurements.

Prakash suggested that thermocouples could be mounted at some known locations far away from the cutting tip. By measuring the temperatures at those locations, the temperature at the cutting tip could be predicted using the model. A control system could then be designed to reduce the cutting speed if the temperatures reach levels in the vicinity of the critical temperature of Polycrystalline Diamond Compacts.

The primary objective of this study is to verify the theoretical model of Prakash experimentally. As suggested by him and others, different methods will be considered

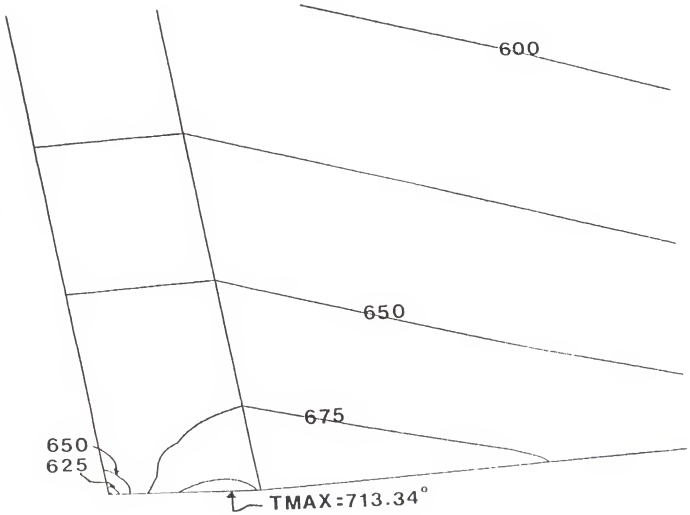

Figure 7: Temperature contours in the tool (Magnified) - Prakash

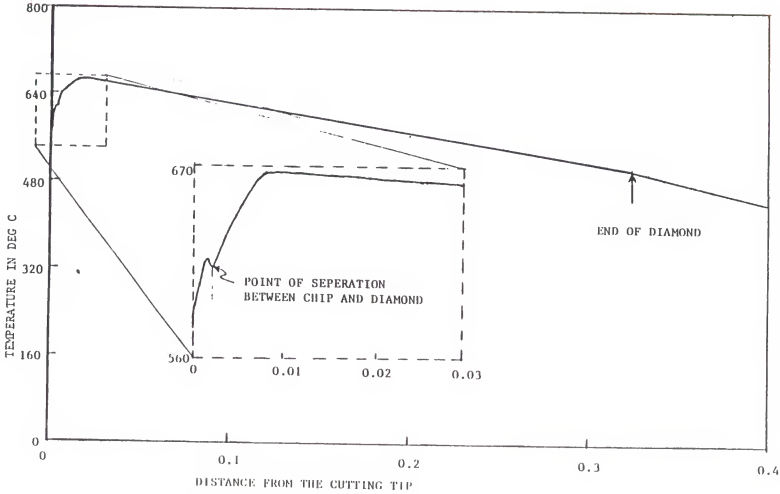

Figure 8: Temperature Distribution along the Rake Face - Prakash

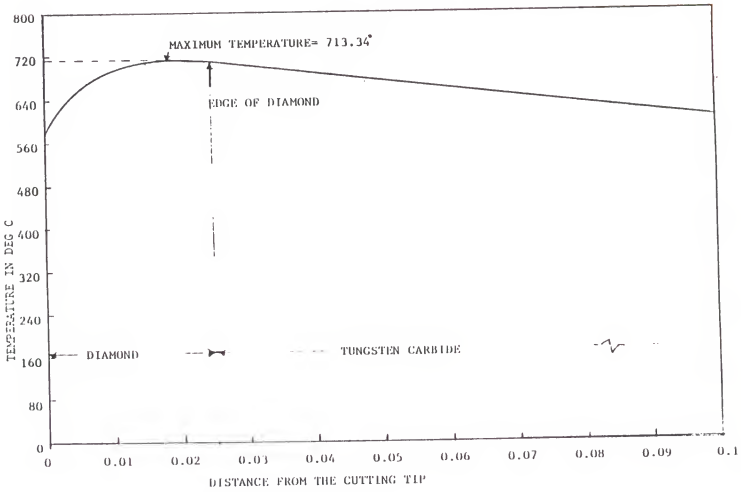

Figure 9: Temperature Distribution along the bottom face - Prakash

for the measurement of temperature. Some of these methods could well be used with MWD and the required systems to control drilling operations.

2.0 METHODS OF TEMPERATURE MEASUREMENT

2.1 Temperature: some basic ideas [3]

Temperature is a quantity which takes the same value in two systems that are brought into thermal contact with one another and allowed to come to thermal equilibrium. This statement on the meaning of temperature provides the basis for thermometry.

Closely linked to the concept of temperature, and often confused with it, is the concept of heat. It is a matter of common experience that some substances require more heat to warm them than do others. Nevertheless, given sufficient insight, common experience allows us to make a number of very fundamental statements about the thermal behavior of matter: these statements comprise the law of thermodynamics. The fundamental law of thermometry, the zeroth law is concerned with the state of bodies brought into thermal contact with one another:

If two systems are separately in thermal equilibrium with a third, then they are in thermal equilibrium with each other.

This may also be presented slightly differently

If three or more systems are in thermal contact with each other and all in equilibrium together, then any two taken separately are in equilibrium with one another.

We can thus imagine one such system, which we call a thermometer, being brought into thermal contact in turn

with other systems to find out whether they are in similar or different thermal states.

Among the thermodynamic parameters which describe the thermal state of systems in equilibrium there is one which has the special property of always taking the same value in different systems which are in thermal equilibrium with each other. It is this one that is called "temperature". Thus all systems in thermal equilibrium with one another have the same temperature.

Several methods of thermometry have been developed in the past three hundred years. Each of these methods have specific applications and advantages. In the next few sections, we will discuss two of these types which are popular in measurement of cutting temperatures, namely thermocouple and infrared temperature measurements.

2.2 Thermocouple temperature measurements [4,5,6]

A thermocouple is a device for the measurement of temperature. Its operation is based upon the findings of Seebeck (1821). His work showed that a small electric current will flow in a closed circuit composed of two dissimilar metallic conductors when their junctions are kept at different temperatures. The electromotive force (emf) produced under these conditions is known as Seebeck emf. The pair of conductors, or thermocouple elements which constitutes the thermoelectric circuit is called a thermocouple. Simply stated, a thermocouple is a device

which converts thermal energy to electric energy. The amount of electric energy produced can be used to measure temperature.

Certain pairs of thermocouple elements give emfs which vary in a regular way with the temperature differences between their junctions. Thermometric use may be made of this behavior by maintaining one of the junctions at a known, fixed, reproducible temperature. This temperature is called the **reference temperature** and, for practical measurements, usually is taken at the melting point of ice (0 deg. C). The junction maintained at such a temperature is known as the **reference junction**; the other junction is called the **measuring junction**. Under normal conditions the reference junction temperature is the ambient temperature at the junction of the thermocouple wire and the copper wire leading to the potentiometer (or the ambient temperature at the binding posts of the potentiometer). This temperature is relatively constant and short-term fluctuations can be ignored. However, where the effects of these fluctuations become significant, such as in an air-conditioned room, or where the highest degree of accuracy is required, one of the following methods can be used to maintain a relatively constant reference junction temperature, independent of ambient temperature fluctuations.

2.2.1 Ice Bath Method

The ice bath maintains the reference junction temperature at 32 deg. F (0 deg. C) in the circuit of Figure 10. Note that the reference junctions are now at the junction of the copper and the thermocouple extension wires, instead of at the emf binding posts. Since the conversion tables are based upon a reference junction temperature of 32 deg. F (0 deg. C), the reference junction compensator is not required in this method.

The ice bath consists of two thermally insulated containers (I.D. 1.5 to 2.5 inches) in which a mixture of compacted, distilled, crushed ice and distilled water surround the reference junctions. The quantity of water used should be limited to the amount necessary to ensure a water-ice mixture, which is the only means of maintaining a true 32 deg. F (0 deg. C) temperature. Care should be exercised when the reference junctions are inserted into the ice bath. At least a four-inch immersion is recommended. The crushed ice should be pressed firmly around the wires.

A single container can be used if the water is of sufficient purity to ensure electrical insulation between the reference junctions. The reference junction wires can also be dipped in melted paraffin to provide the required insulation.

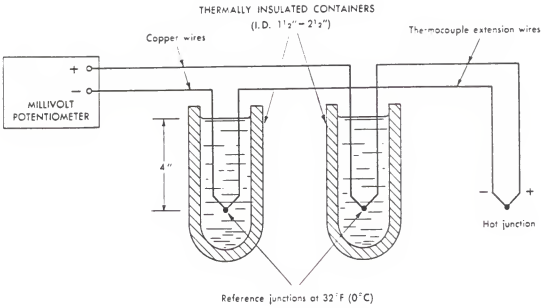

Figure 10 - Ice bath circuit

2.2.2 Thermal Insulation Method

A less precise but satisfactory method of maintaining a stable reference junction temperature is to embed the junctions in a mass of thermal insulating material, such as foamed polystyrene. The reference junction temperature is determined by a mercury thermometer embedded with the junctions. In this method, the reference junction temperature is relatively constant in spite of room temperature fluctuations. However, the difference in temperature between the reference junction and 32 deg. F (0 deg. C) must be compensated for by the reference junction compensator.

Most thermocouple thermometers commercially sold are available with built-in cold junction compensating circuits without the need for a separate reference junction. The Doric 403 Trendindicator and 405A Multipoint Selector combination used for this study has similar auto cold junction compensation.

When a reference temperature (or cold junction compensation) is used, the temperature difference, and consequently the emf of a thermocouple, becomes a function of the temperature of the measuring junction (hot junction). The functional dependence permits the establishment of tables, curves, or mathematical relationships, which in turn, provide the emfs generated by various pairs of thermocouple elements in terms of the

temperature of the measuring junction. This is the general approach followed in thermoelectric thermometry.

2.3 Laws of Thermoelectric Circuits

2.3.1 Law of Homogeneous Materials

A thermoelectric current cannot be sustained in a circuit of a single homogeneous material, however it varies in cross section, by the application of heat alone.

A consequence of this law is that two different materials are required for any thermocouple circuit.

2.3.2 Law of Intermediate Materials

The algebraic sum of the thermoelectromotive forces in a circuit composed of any number of dissimilar materials is zero if all of the circuit is at a uniform temperature.

A consequence of this law is that a third homogeneous material can always be added in a circuit with no effect on the net emf of the circuit as long as its extremities are at the same temperature. Therefore it is evident that a device for measuring the thermoelectromotive force may be introduced into a circuit at any point without affecting the resultant emf, providing all the junctions that are added to the circuit by introducing the device are at the same temperature (Figure 11). It also follows that regardless of the method employed in forming the junction (e.g., solder, braze, or crimp), the emf of the thermoelectric circuit is unaffected so long as the

temperature of the junction is uniform and that good electrical contact is assured.

Another consequence of this law may be stated as follows. If the thermal emfs of any two metals with respect to a reference metal are known, the emf of the combination of the two metals is the algebraic sum of their emfs against the reference metal (Figure 12).

2.3.3 Law of Successive or Intermediate Temperature

If the two dissimilar homogeneous materials produce a thermal emf of E_1 when the junctions are at temperatures T_1 and T_2, and a thermal emf of E_2 when the junctions are at T_2 and T_3, the emf generated when the junctions are at T_1 and T_3 will be $E_1 + E_2$ (Figure 13).

One consequence of this law permits a thermocouple calibrated for a given reference temperature to be used with any other reference temperature through the use of a suitable correction.

Another consequence of this law is that extension wires having the same thermoelectric characteristics as those of the thermocouple wires can be introduced in the thermocouple circuit (say, from region T_2 to region T_3 in Figure 13) without affecting the net emf of the thermocouple.

In summary, we need understand neither the complexities of electron-photon interactions nor the exact location of the seats of emf in a thermocouple circuit to

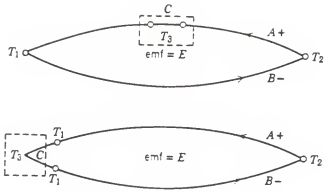

Figure 11 - The emf is unaffected by the third material C

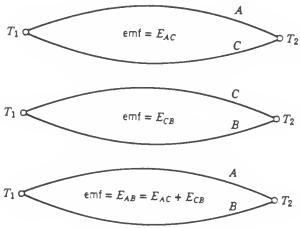

Figure 12 - Emfs are additive for materials

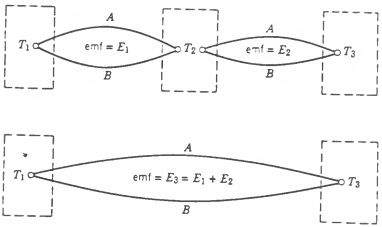

Figure 13 - Emfs are additive for temperature intervals

use a thermocouple successfully. We need only heed the laws of thermoelectricity. Stated more succinctly, we must understand that thermoelectric emfs are generated only in regions of temperature gradients and that thermocouple errors, arising from nonuniformities in circuit components, can occur only in regions of temperature gradients.

2.4 Elementary Thermoelectric Circuit

Two continuous dissimilar (Chromel-Alumel) thermocouple wires extending from the measuring junction to the reference junction, when used with copper connecting wires and a potentiometer connected as shown in Figure 14, make up the basic thermocouple circuit. This is the arrangement that has been used in our study.

2.5 Thermocouple Reference Tables

Thermocouple reference values represent in both form and magnitude the nominal characteristics of particular thermocouple types. Thermocouple wires are carefully selected and matched to conform with these tables within prescribed limits. The printed scales of all direct temperature-indicating potentiometers are based on such tables. Calibration curves, in the form of voltage or temperature difference plots are obtained by comparing calibration data with reference values.

Figure 15 shows temperature versus emf curves for different pairs of thermocouple materials. Chromel-Alumel

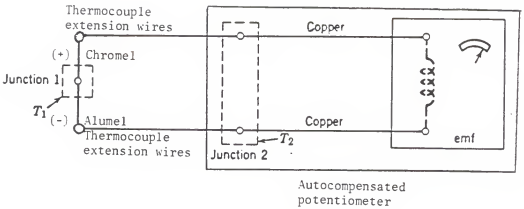

Figure 14 - Basic thermocouple circuit using K type

Table 1 - Power series expansions for Type K thermocouples

Temperature Range (°C)	Exact Reference Voltage (mV) E	Reference Temperature T
	Type K Thermocouples	
		Within ±0.02°C
0 to 400	$(-1.8533063273 \times 10$ $+3.8918344612 \times 10 \times T$ $+1.6645154356 \times 10^{-2} \times T^2$ $-7.8702374448 \times 10^{-5} \times T^3$	No inverse equation available to a reasonable degree of accuracy
400 to 1100	$+2.2835785557 \times 10^{-7} \times T^4$ $-3.5700231258 \times 10^{-10} \times T^5$ $+2.9932909136 \times 10^{-13} \times T^6$ $-1.2849848789 \times 10^{-16} \times T^7$ $+2.2239974336 \times 10^{-20} \times T^8$ $+125 \exp\left(-\frac{1}{2}\left\{\frac{T-127}{65}\right\}^2\right)\Big) \times 10^{-3}$ (applies to both ranges of temperature)	-2.4707112×10 $+2.9465633 \times 10 \times E$ $-3.1332620 \times 10^{-1} \times E^2$ $+6.5075717 \times 10^{-3} \times E^3$ $-3.9663834 \times 10^{-5} \times E^4$

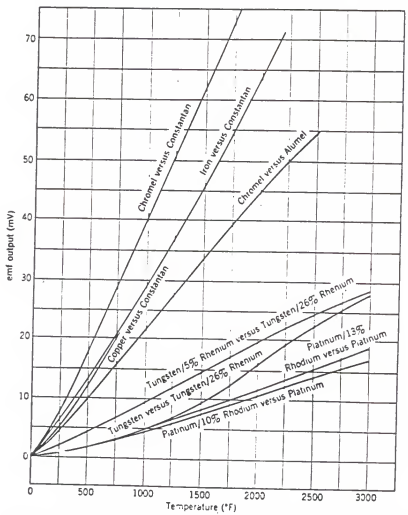

Figure 15 - Temperature versus emf curves. Reference junction, 32 deg. F

thermocouple (K type) was selected in our research for the following reasons:

i. Readily available in foil form to enable surface temperature measurements, and

ii. Temperature range (0 - 800 deg. C) suits our application.

2.5.1 Type K (Chromel-Alumel)

Outputs of these thermocouples can be represented by the equation in Table 1. An eighth degree equation with an exponential term is used to generate values of voltage as a function of temperature from 0 to 1372 deg. C. The inverse relation provides reference temperatures accurate to +/-0.02 deg. from 400 to 1100 deg. C.

Conversion tables for K type thermocouples on the Celsius and Fahrenheit scales respectively are shown in Appendix A.

2.6 Introduction to Infrared Radiation

All objects emit infrared radiation. Infrared energy is generated by the vibration and rotation of atoms and molecules within a substance. As an object becomes hotter, its molecular activity increases and causes that object to generate more energy. Only at absolute zero (-273 deg. C), where all molecular activity stops, will an object cease to emit infrared radiation.

Infrared radiation, like radio waves, light, and x-ray radiation, is electromagnetic and travels through

space at the speed of light. The infrared spectrum has wavelength in the range 0.7 - 1000 micrometers.

Infrared radiation obeys many of the laws that apply to light. Materials have properties of reflectivity, absorptivity, and transmissivity toward infrared just as they have for light.

2.6.1 Stefan-Boltzmann Law

The hotter an object becomes, the more infrared energy it emits. The following formula shows the relationship between the total energy emitted by an object and its temperature:

$$W = (E)(s)(T^4)$$

where,

W equals radiant energy in watts per square centimeter,

E equals emissivity factor,

s equals Stefan-Boltzmann constant (5.67×10^{-12} W/cm^2K^4),

T equals temperature in deg. kelvin.

2.7 Infrared Detectors

The main component in any infrared system is the detector. The detector is used to convert radiant energy into an electrical signal that may be used to provide a variety of desired readouts.

There are many types of infrared detectors. Each type has a distinct set of operating parameters, or

characteristics. Some of the more important characteristics are as follows:

2.7.1 Signal (S)

The signal (S) is the voltage generated by an infrared detector that is related to the infrared energy striking that detector. The signal generated by an infrared detector may vary with detector size, temperature, bias, and time constant.

2.7.2 Responsivity (Rv)

Responsivity (Rv) is the ratio of signal output to incident radiant flux. It is usually expressed as volts per watt and may be written as

$$Rv = (S/J)$$

where,

Rv equals responsivity,

S equals rms voltage from detector,

J equals rms value of energy flux striking the detector.

2.7.3 Noise (N)

Noise (N) is the voltage generated by an infrared detector as a result of its resistance, temperature, bandwidth, and bias. Noise is independent of signal input. Cooling the detector decreases its noise voltage and therefore increases its S/N ratio and detectivity.

2.7.4 Signal-to-Noise Ratio (S/N)

The S/N ratio is the ratio of signal to noise. The

higher the S/N ratio, the better the detector.

2.7.5 Noise Equivalent Input (NEI)

The noise equivalent input (NEI) is the amount of incident radiation (measured in watts per square centimeter) on an infrared detector that will produce a signal/noise ratio of 1. Mathematically,

$$NEI = (J)(N)/(S)$$

where,

J equals rms incident energy flux,

N equals rms noise voltage,

S equals rms signal voltage.

2.7.6 Noise Equivalent Power (NEP)

The noise equivalent power (NEP) is similar to NEI except the incident energy is measured in watts rather than watts per square centimeter. It may be expressed as

$$NEP = (J)(N)(A)/(S)$$

where,

NEP equals noise equivalent power in watts,

J equals rms incident energy flux in watts per square cm,

N equals rms noise voltage,

S equals rms signal voltage,

A equals area of detector element.

2.7.7 Detectivity (D)

The detectivity (D) is the reciprocal of NEP.

2.7.8 Time Constant

A time constant is the time required for a signal to build up to 63 percent of its maximum. The frequency response of an infrared detector is dependent on its time constant.

2.8 Types of Detectors

Infrared detectors fall into two major categories: thermal and quantum detectors.

Operation of the thermal detector is based on the change of a physical property (such as resistance or thermoelectric force) of the detector as its own temperature is changed. Some common examples of thermal detectors are thermocouples, pneumatic detectors, and bolometers.

A quantum detector is a semiconductor that produces a signal proportional to the photon flux that strikes its sensitive element. Quantum detectors include photoconductive, photovoltaic, and photoelectromagnetic detectors.

In general, thermal detectors have a uniform spectral response but exhibit a longer time constant than quantum detectors.

2.8.1 Thermal Detectors

Thermocouple - One junction of the thermocouple is generally flattened into a disc and blackened to improve its absorption of incident radiation. The other junction

is shielded from incoming radiation and forms part of an electrical balanced bridge circuit to offset the effects due to changes in ambient temperature.

Thermopile - A series of thermocouples is called a thermopile. Thermopiles generate larger voltage potentials, for a given temperature, than thermocouples.

Metal Strip Bolometers - Metal bolometers are blackened strips of thin metal having a low heat capacity and a high temperature coefficient of expansion. Changes in resistance across the bolometer strip occur as the incident energy is changed.

2.8.2 **Quantum Detectors**

Quantum detectors are semiconductors that essentially count the amount of photons striking a sensitive element. Photons striking a quantum detector interact with the crystal lattice, freeing electrons or holes.

There are three photon detection techniques: photoconductive, photovoltaic, and photoelectromagnetic.

The photoconductive effect is the increase in electrical conductivity of a semiconductor caused by an increase in free carriers produced by incident radiation.

The photovoltaic effect takes place at a pn junction in a semiconductor. Photons striking the junction cause hole-electron pairs to diffuse in opposite directions across the junction, producing a charge separation and therefore a voltage.

The photoelectromagnetic effect is also a diffusion phenomenon that occurs when radiation falls upon a semiconductor that is within a magnetic field.

Lead Sulfide - The lead sulfide (PbS) detector is perhaps the most common of all infrared photoconductive detectors. Lead sulfide detectors may be chemically deposited or evaporated onto a substrate (usually quartz). Lead Sulfide detectors may be operated at room temperatures or may be cooled to increase their S/N ratios.

Lead Selenide - Lead Selenide (PbSe) detectors are photoconductive and may be produced in much the same way as lead sulfide.

Indium Antimonide - Perhaps the most versatile of all infrared detectors, indium antimonide (InSb) may be used as a photoconductive, photovoltaic, or photomagnetic detector.

2.9 Optics

All infrared systems require a transmitter and a receiver. Optics may be used at the transmitter to shape, direct, or modify the infrared radiation before it reaches the receiver. The receiver may use optical techniques to help collect and focus the incoming radiation onto an infrared detector. As mentioned earlier, infrared radiation follows all the laws of geometrical and physical optics, viz. reflection, refraction, interference,

diffraction, and polarization.

2.9.1 Materials

Optical materials are selected based on their properties such as Index of Refraction, hardness, solubility, thermal expansion, melting temperature and thermal conductivity.

2.9.2 Fiber Optics

Some smooth transparent rods transmit visible and infrared energy by multiple internal reflections. This phenomenon is called total internal reflection. Transmission of light can also take place in a very small diameter rod such as a fiber.

A portion of the energy entering a fiber will emerge from the opposite end. The loss in transmission is due to the absorption of the transmitting media, scattering, and end-surface reflection.

The transmission of a fiber is increased by coating a high-refractive index core with a substance of low refractive index.

2.10 Instrumentation

2.10.1 Radiometers

An infrared radiometer is a device used to measure the amount of thermal energy radiated by a substance. The radiometer is the most common and most basic of all infrared instruments and systems. There are many types and designs of infrared radiometers but they all contain

the same basic components.

Basic Radiometer

Figure 16 shows a simplified block diagram of a typical infrared radiometer. The solid blocks indicate the components, or circuits, required for a basic radiometer. The remaining blocks indicate additional circuits that may be added to increase the instrument's overall abilities.

Optical System - Optical systems are used to collect and focus the infrared energy into the detector. The optical system acts as an amplifier since it permits the relatively small infrared detector to "see" higher levels of infrared radiation.

Optical systems may be refractive or reflective, or simple or complex, depending on the application. Major considerations in choice of optical systems are wavelengths to be measured and field of view, which depends on target size and distance.

Modulator - The infrared detector in a radiometer normally looks at a target that has a constant or slow-changing temperature. This results in a very-low-level dc signal from the detector which is difficult to amplify. Detector outputs of a few microvolts are common.

A chopper blade may be used to modulate the incoming radiation at a fixed frequency. This produces an ac signal which is easier to amplify.

Infrared Detector - The infrared detector is the "heart" of a radiometer. The detector alternately "sees" the energy emitted from the chopper blade and then the energy emitted from the target. In this case the chopper blade temperature becomes the reference level. The amplitude of the ac signal from the detector is related to the difference between the temperature of the chopper blade and that of the target.

Built-in Calibration - The accuracy of any instrument depends somewhat upon its calibration. Radiometers are generally calibrated in the laboratory by use of black body radiation sources. In many radiometer applications it is impractical to use laboratory calibration techniques. For this reason, some radiometers have a built-in calibration source.

2.10.2 Infrared Thermometers

Infrared thermometers are radiometers used for temperature measurement and control. Most infrared thermometers are relatively simple compared with more sophisticated radiometers.

Typical Infrared Thermometer

Figure 17 shows a simplified diagram of a typical radiometer used for general-purpose, noncontact, temperature measurement. The incoming radiation is collected by a glass or quartz lens and focused onto a lead sulfide detector. A dichroic beam-splitter transmits

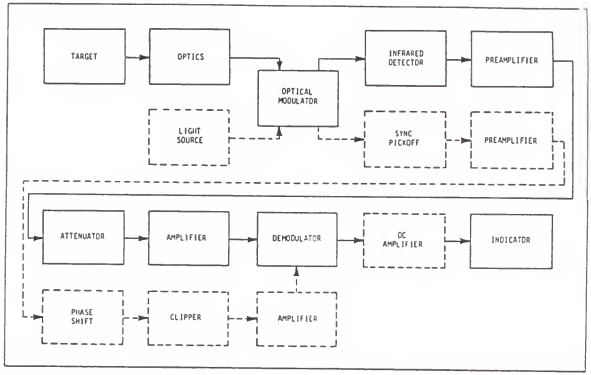

Figure 16 - Block diagram of infrared radiometer

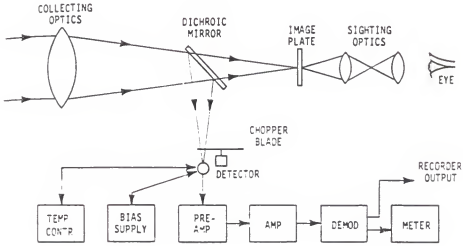

Figure 17 - Radiometer for temperature measurement

the visible signal to the on-axis sighting optics and also deflects the infrared energy to the detector. A fixed-frequency chopper blade driven by a synchronous motor modulates the incoming radiation at about 300 hertz. Focusing from a few feet to infinity is accomplished by moving the lens along the optical axis. The target is focused onto an image screen that is at the same distance from the lens as that of the detector. The image screen usually contains a reticle that defines the radiometer field of view so that the user knows whether or not the target is resolved.

Spectral response of this type of radiometer is usually from 1.0 to 2.7 micrometers. Within this spectral band, temperatures as low as 200 deg. F can be detected. Extremely high temperatures will require the use of optical attenuators to prevent the detector from saturating or heating.

The lead sulfide detector is heated to a temperature of at least 130 deg. F for stability and for reliable operation in ambient temperatures up to the detector control temperature.

Specifications of a typical infrared thermometer are as follows:

Temperature Range:	200 to 5000 deg. F
Temperature Accuracy:	2% of temperature
Temperature Sensitivity:	0.5% of temperature

Temperature Repeatability:	0.5% Of temperature
Focusing range:	10 inches to infinity
Field of View:	1 deg.
Spectral Response:	1.0 to 2.7 micrometers
Emissivity Range:	0.2 to 1.0

Temperature measurement and control by infrared techniques is used in virtually every industrial process. Infrared radiometers provide quick, remote temperature measurement without affecting the temperature of the object being observed. Operation of the radiometer is simple. Just aim the unit, like a camera, and read the temperature. Most radiometers have an emissivity adjustment for absolute temperature readings. Radiometers generally have a recorder output for pen recorders or for temperature controllers.

Commercial Equipment

Vanzetti Systems, Massachusetts are manufacturers of infrared thermal monitors for non-contact temperature measurements. These monitors are specially designed for applications involving hostile environments - where extremes of heat, voltage, radiation, or corrosion make conventional methods difficult or impossible. The key is the integration of fiber optics to monitor infrared radiation. An IR "pipe" - a single fiber or several fibers in bundle construction depending upon the application - gathers the radiation, which is a function

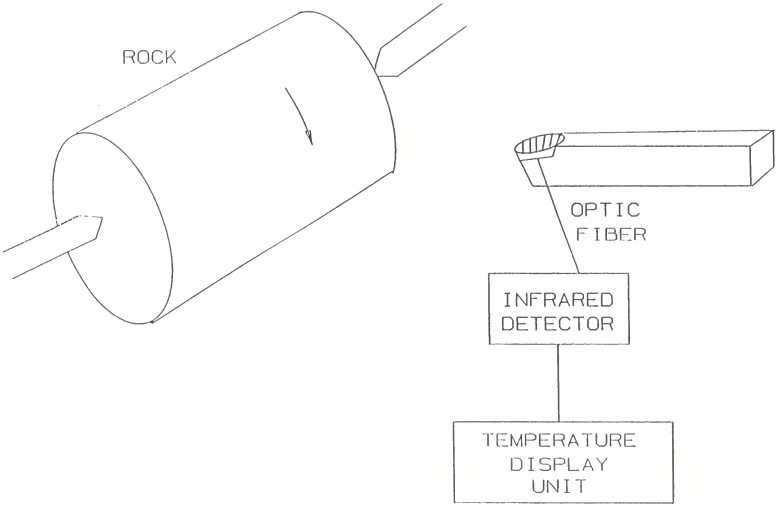

Figure 18 - Proposed setup for infrared measurement of temperature

of temperature, and transmits it to a console where it is converted to a voltage suitable for digital display, recording, or interfacing with other control and data processing systems. The system consists of three major components: the fiber optic assembly; an infrared sensor; and an electronic console. The infrared sensor contains a photon detector, encased in a rugged remotely-mounted enclosure. The interconnecting cable to the control console can be over 30 feet long when necessary. The fibers are made of infrared transmitting glass consisting of a transparent core coated with a thin film of cladding glass of lower refractive index to provide a viewing angle of approximately 60 deg. at the tip. Optional lenses may be used for smaller angles. Special ceramic-encased fiber optic tips can be used for precise thermal measurements in ambient temperatures as high as 1000 deg. C.

A Vanzetti 4 channel infrared thermal monitor with temperature range 400-800 deg. C. costs about $14,000.

Proposed infrared experimental setup

Figure 18 shows the proposed setup for measuring tool temperatures using fiber optics and infrared detection.

3.0 CUTTING TEMPERATURE MEASUREMENTS METHODS AND LITERATURE SURVEY

3.1 Methods of tool temperature measurement

The difficulty of calculating temperatures and temperature gradients near the cutting edge, even for very simple cutting conditions, gives emphasis to the importance of methods for measuring temperature [7]. This has been an important objective of research and some of the experimental methods explored are now discussed.

3.1.1 Tool-work thermocouple

The most extensively used method of tool temperature measurement employs the tool and the work material as the two elements of a thermocouple. The thermo-electric emf generated between the tool and work piece during cutting is measured using a sensitive millivoltmeter. The hot junction is the contact area at the cutting, while an electrical connection to a cold part of the tool forms the cold junction. The tool is electrically insulated from the machine tool (usually a lathe). The electrical connection to the rotating workpiece is more difficult to make, and various methods have been adopted, a form of slip-ring often being used. The tool-work thermocouple is calibrated using a standard thermocouple for each tool and work material used.

The use of this method requires that the work material should be electrically conductive. Since the

work material in our study is rock which does not satisfy this condition, we will not discuss this method any further.

3.1.2 Embedded thermocouple

Measurement of the distribution of temperature in the tool has been the objective of much experimental work. Thermocouples embedded in cutting tools have been used to measure cutting temperatures. A simple but very tedious method is to make a hole in the tool and insert a thermocouple in a precisely determined position close to the cutting edge. This must be repeated many times with holes in different positions to map the temperature gradients. Figure 19 is an example of such a study. The hole in which the thermocouple is placed represents a disturbance and may appreciably change the temperature field being measured unless it is very small [8]. The main error in this method arises because the temperature gradients near the edge are very steep, and holes large enough to take the thermocouple overlap a considerable range of temperature. Small holes are usually made by electroerosion.

3.1.3 Radiation methods

Several methods have been elaborated for measurement of radiation from the heated areas of the tool. In some machining operations, the end clearance face is accessible for observation, for example in planning a narrow plate.

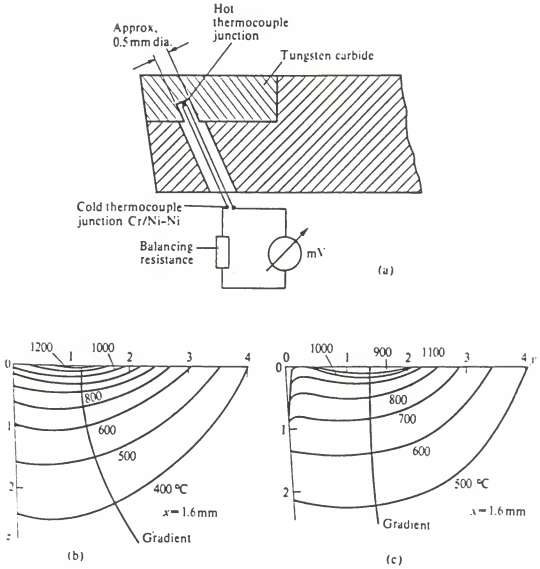

Figure 19 - Embedded thermocouple technique for mapping temperatures in cutting tool used in turning operation. (M.C.Shaw)

(a) Experimental arrangement

(b) Sharp tool

(c) Worn tool

The end clearance face may be photographed, using film sensitive to infrared radiation. It is also possible to measure the infrared radiation from the tool, work, and chip in orthogonal cutting to establish the temperature field on the outside surfaces of these regions. While this method does not reveal internal temperatures, it does provide a valuable early insight into the temperature distribution on the shear plane, tool, and chip.

The main difficulty with radiation techniques is that they are generally limited to accessible surfaces. To overcome this, a more refined but difficult technique is used. This technique involves making holes, either in the work material or in the tool to act as windows through which a small area (e.g. 0.008" dia.) on the rake surface of the tool can be viewed. The image of the hot spot is focused onto a infrared detector (PbS photo-resistor/photo diode) which can be calibrated to measure the temperature. By using tools with holes at different positions, a map can be constructed showing the temperature distribution.

3.2 Literature survey

The problem considered by Boothroyd [9] was the determination of the temperatures generated in the workpiece, chip, and tool during orthogonal metal cutting. He considered the temperatures generated along the rake face of the tool to be of the greatest interest since they were thought to affect both the rate of wear of the

cutting tool and the friction between the chip and tool. In his experiment, a pre-heated tubular workpiece was end-machined in a lathe and the cutting operation and a small heated strip of metal (used for calibration purposes) were photographed simultaneously. An infrared photographic plate was used, and because the temperature distribution along the heated strip could be obtained from thermocouple readings, the optical density of the plate, after processing, can be calibrated against the temperature. Using a microdensitometer to explore the variations in optical density of the plate, it was possible to plot the temperature distribution in the workpiece, chip, and tool.

Wright [10] describes metallographic experimental methods to measure the temperature gradients in cutting tools. In his earlier work, an experimental method was described for determining the temperature gradients in BM34 high-speed steel cutting tools over the range 600 to 1000 deg. C. Metallurgical examination of sections of worn tools showed that the heat conducted into the tool could permanently alter the temper of the steel if temperatures were greater than the secondary hardening temperature of 560 deg. C. These tempered structures were evident after etching in 2% nital for 30 seconds and also could be resolved by microhardness testing. To correlate such effects with temperature (and time) it was necessary to prepare standard specimens from thin samples

of the BM34 high-speed steel that were heat treated in a salt bath at 550 deg. C and above. The hardness and microstructure of these specimens were then related to those in the tools by assuming that the heating cycle from a standard cutting time, say 60 seconds, was the same as the heating cycle of the thin specimen immersed in the salt bath for 60 seconds.

Triemel and Panhorst [11] conducted studies in heat generation and temperature measurement in diamond machining operations. The objective was to assess and explain diamond wear phenomena. This paper explains qualitatively the generation of heat at the contact area between abrasive grit and workpiece, and describes the practical difficulties in measuring the temperature. Triemel and Panhorst mention that measurement of forces can be done with little possibility of error, and so can the wear. Temperature measurement, on the other hand, inevitably seemed to involve a high incidence of error, and exact figures for temperatures in the diamond abrasive/workpiece contact area were not obtainable. Various techniques developed previously for temperature measurement were analyzed. Theoretically all the measurement techniques shown in Figure 20 are applicable to diamond machining; however, only a proportion of these were proved capable of practical adaptation.

The thermoelectric effect, according to them, is used by

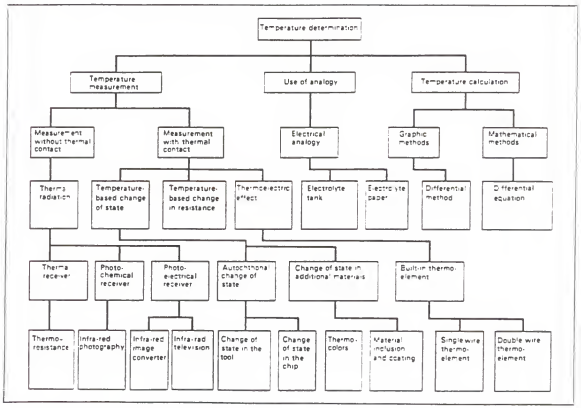

Figure 20 - Method of determining temperatures during diamond machining

the vast majority of temperature measurement techniques. They refer to an interesting thermoelectric measuring technique in which a platinum wire is embedded in the workpiece as the thermocouple for measuring temperatures at the workpoint. The thermal wire is insulated and mounted between two workpiece clamps. A groove is ground into one clamping bar normal to the direction of cut (Figure 21) in order to prevent damage by the clamping. The hot end is formed by grinding the workpiece, when the platinum wire is smeared over the workpiece surface; the cold end is outside the contact area on the workpiece. This method permits, to a limited degree, measurement of the individual temperature rises brought about by the abrasive particles taking part in the machining process.

Triemel and Panhorst also describe grinding temperature measurement by thermal radiation. The measuring instruments which are used register the infrared radiation emitted by the heated object, and, with a suitable scale of measurement, a definite temperature can be ascribed to the radiation level. In the method described to measure temperature and heat flow (Figure 22), holes are drilled into the grinding wheel face at an angle to the surface line, and a 'photo-resistance' is placed over the exit points of each hole. As the wheel rotates, a hole, ie. radiation channel and photo-resistance, is covered up briefly, the radiation energy

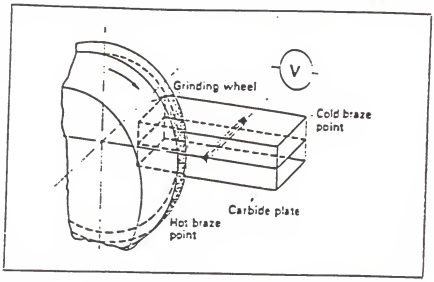

Figure 21 - Thermoelectric measurement of the grinding temperature

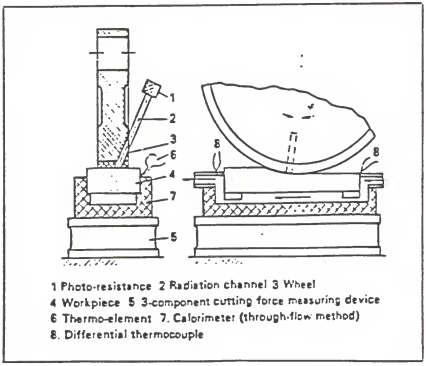

Figure 22 - Temperature and heat flow measuring equipment (Triemel etal)

impulse strikes the photo-resistance and causes a reduction in its resistance, which provides a basis for the determination of temperature in the contact zone. This method makes it possible to measure temperature directly in the contact zone with little phase shift (0.0001 seconds), and can also be used on non-conducting workpieces. It has, however, the disadvantage that preparatory machining work has to be done on the tool.

Barrow [12] categorizes methods of measuring cutting temperature (both average values and distribution) as follows:

a) Thermo-e.m.f. (thermocouples).

b) Radiation (pyrometry, infrared photography, etc.).

c) Thermo-chemical reactions (thermo-colors).

Barrow describes thermo-e.m.f. measurements using embedded thermocouples. With this technique there are two basic techniques, those monitoring the temperature at a single point (this may or may not be the point of maximum temperature) and those attempting to obtain a two or three dimensional temperature distribution.

The most commonly used method has been the insertion of a standard thermocouple either in the workpiece at some distance from the tool face or at the interface between chip and tool. When the thermocouple is in the workpiece, the temperature can be measured at any point in the direction of chip flow, temperatures on the tool face

being obtained by extrapolation. The problems associated here are the interference to heat flow caused by the embedded thermocouples, inaccuracies in extrapolation, response time of thermocouples and in the case of thermocouples at the interface, the effect of the 'rubbing' conditions.

Barrow also describes the infrared photography technique developed by Boothroyd. The main disadvantage of this technique according to him is the limiting sensitivity of the photographic plates used. This resulted in limiting the range of temperatures which could be measured to between 500 and 700 deg. C.

The use of thermosensitive paints for estimating cutting temperature utilizes the fact that these paints change color at certain temperatures. Their use is restricted to accessible surfaces, there is a relatively long time lag for the colors to change and small changes in temperature are difficult to detect.

The study of Kazuaki etal [13] aims at understanding the ultra-high precision machining process and developing relevant technologies. The ultra-high precision cutting of copper (OFC) was carried out employing diamond tools on an ultra-high precision fly cutting milling machine equipped with an ultra-high precision spindle supported by hydrostatic air bearings. The thermal electromotive forces generated in the thermocouple of the copper

workpiece and the constantan wire, which was specially inserted within the workpiece, were recorded by a digital storage oscilloscope or a pen recorder. The cutting tool was attached to the cutter body through acrylic resin insulator in order to prevent the noise signal.

Panhorst and Triemel [14] used a miniature thermocouple for measuring temperatures during grinding. 'Scratch' tools tipped with single particle diamond or corundum were used. The crystals were drilled by means of a laser beam and ultrasonics to permit installation of the chromel/alumel thermocouple as close as 0.3 mm from the particle's contact face with the workpiece surface (Figure 23). The small dimensions of the thermocouple which had a radius of .125 mm at the measurement point, produce a relatively low time constant of 6 milliseconds.

Harris, Hastings, and Mathew [15] used infrared thermography technique based on commercial closed circuit television components to measure tool and workpiece temperatures during cutting. A technique based on radiation measurement was selected as the most suitable because of its non contacting nature and its ability to provide complete temperature fields. An infrared sensitive vidicon was used as the temperature detector. This method relies on converting the TV picture in to photographic images which are subsequently analyzed with a photodensitometer. Infrared images were first recorded on

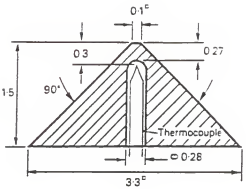

Figure 23 - Location of miniature thermocouple in the cutting particle

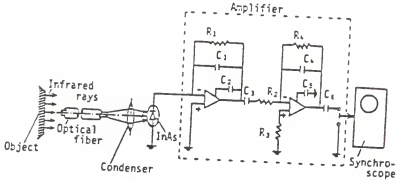

Figure 24 - Pyrometer system used by Ueda, Hosokawa and Yamamoto

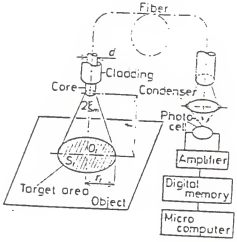

Figure 25 - Fundamental measuring system with optic fiber

video tape and then replayed for analysis. This step was necessary because of the short duration of each cutting test and the need to select a frame in which the field of view is not obstructed or affected in any way by chips, sparks, fragments etc. The system was first calibrated by recording images of a piece of heated tungsten carbide rod. An attached thermocouple was used to record the temperature of the radiating surface and this information was later used to relate the recorded image intensities to actual temperatures.

Various techniques of infrared radiation measurements were investigated by Kops and Shaw [16] to provide a new insight into grinding mechanics, based on thermal radiation. The usefulness of high speed infrared films, lead sulfide photocells and a thermovision system were tested in a number of grinding experiments. The experiments were conducted using both photographic films and photocells. The usefulness of various infrared radiation detectors was tested in a number of grinding experiments. These include: grinding with a single abrasive particle, special contoured wheels and a conventional disc shaped wheel operating in surface grinding mode. A calibration setup consisting of an embedded thermocouple in a grinding wheel was proposed.

Ueda, Hosokawa, and Yamamoto [17] used a new method to measure temperature of cutting grains on a grinding

wheel surface. They used an optical fiber which accepted the infrared flux radiated from the cutting grains after they exit from the cut and transmitted it to an infrared detector InAs cell. This pyrometer made it possible to track each cutting grain on the wheel surface and is suitable for measuring the temperature of a very small object whose temperature changes rapidly. The fiber can enter into an intricate part because it is freely yielding and can accept the infrared rays radiated from a very small area. It is therefore easy to measure the inside temperature of the object by drilling a microscopically fine hole in it to insert the fiber. The schematic illustration of the infrared radiation pyrometer used by them is shown in Figure 24. The infrared detector InAs cell is kept at 77 deg. K by the use of liquid nitrogen in order to achieve high sensitivity. The electric signal converted from infrared energy by this cell is amplified and observed on a synchroscope screen.

Influence of Setting Location of Fiber on Output Intensity of Pyrometer

Figure 25 shows a fundamental measuring system of infrared radiation pyrometer with optical fiber used by Ueda etal. The core was made up of fluoride glass and surrounded by teflon. Air was used as the cladding material between the core and the teflon. The fiber transmits only those rays which are incident on its face

with an angle less than the acceptance angle ζ_m by total internal reflection at the core-cladding interface. The value ζ_m depends on the ratio of the refractive index of the core and cladding. Therefore the target area and the acceptable energy are influenced by the setting location of the fiber face. The target area S_t when the fiber is placed vertically at a distance of t from the object is expressed by

$$S_t = (t \tan \zeta_m + d/2)^2 \pi$$

where d is the acceptance angle. The fiber can accept only rays radiated from S_t.

The surface grinding was carried out at a constant wheel depth of cut without grinding fluids. The experimental arrangement is illustrated schematically in Figure 26. A fiber (about 2 meters in length) was inserted into the fiber holder mounted beside the wheel. (Its position could be adjusted to any point around the circumference of the wheel.) The chosen position was at an angle of 45 degrees after the cutting point, because it was difficult to distinguish between the pulses from sparks and those from cutting grains at the ideal position which is the cutting point (angle = 0 degrees). The incident face of the fiber was set up by micrometer at a distance of .1 mm from the wheel surface. Therefore the target diameter was about 0.097 mm. The output voltage generated was stored in the digital memory and reproduced

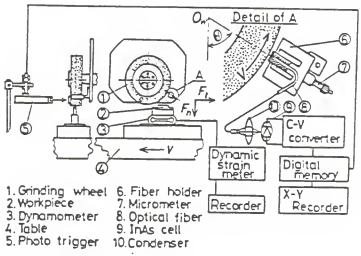

Figure 26 - Experimental arrangement (Ueda etal)

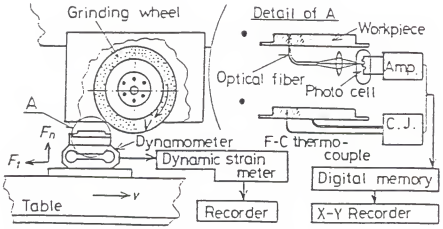

Figure 27 - Experimental arrangement (Ueda etal)

on the X - Y recorder. Calibration of the pyrometer system was done using a K type (Chromel-Alumel) thermocouple.

Figure 27 shows yet another experimental set-up employed by Ueda etal [19]. The optical fiber was inserted into a small hole (its diameter is approximately 0.4 mm) which extends nearly to the base of the hole. If there is a small distance between the incidence face of the fiber and the bottom of the hole, this does not influence the measurement accuracy because the area of the bottom of the hole is larger than the area of the fiber. The fiber can accept the infrared rays radiated from the bottom, when the grinding wheel passes above it. One pass grinding was continued until the bottom of the hole was ground through. The grinding temperature was also measured by means of a thermocouple at the bottom of a small hole of 0.4 mm diameter. It was observed that the infrared pyrometer system had a superior response speed when compared with the thermocouple system. The I.R.P., using an InAs as a detector had a response time in the order of micro-seconds, could detect heat pulses with great accuracy and its signal trace versus time had many sharp peaks. On the other hand, the thermocouple system inferior in response speed, and less accurate in registering heat pulses produced a smooth signal trace versus time curve without any peaks.

4.0 EXPERIMENTAL ARRANGEMENT

Experimentation for temperature measurement was done in two stages, namely, metal cutting and rock cutting.

4.1 Metal Cutting

Metal cutting temperature measurements were done to gain experience before taking up rock cutting. In this experiment dry machining was done on AISI 1020 steel cylinder using standard triangular tungsten carbide inserts TNG-422 with a standard tool holder. The experiment was done for two positions of the K type thermocouple used. Figures 28 and 29 show hole positions used for positioning thermocouple in Experiment #1 and #2. Hole drilling in tungsten carbide was done using EDM (Electrical Discharge Machining) with a brass wire of 1/16" diameter. The resulting drilled hole diameter was 0.070". Several holes were drilled by EDM and the results proved highly repeatable. Drilling was also done using 1/32" diameter brass wire which resulted in a hole of 0.035" diameter. Figures 30 and 31 show arrangements used for Experiment #1 and #2.

Following are the characteristics of Experiments #1 and #2:

Experiment #1:

Feed: 0.010 ipr

Depth of Cut: 0.015"

Experiment #2:

Feed: 0.010 ipr

Depth of Cut: 0.0075"

4.2 **Rock Cutting**

Figure 32 shows the tool holder and parts which go with it. The objective of this tool holder is to reuse a worn circular PDC insert by indexing within the 0.535" diameter hole. The hole in the base and the relief in the clamp act as thermocouple inlets. Many such holes can be provided if temperature sensing is required at different spots on the tool.

A standard K type 0.0005" foil thermocouple (made by RdF corporation), was securely glued on to the PDC insert below the relief in the clamp with glass wool as padding material. *Omega CC high temperature cement* was used as the adhesive since it is capable of withstanding upto 2000 deg. C.

The output signals of the thermocouple were fed into a Doric 403 Trendindicator and 405A Multipoint Selector combination with cold junction compensation which displayed the measured temperature. This unit was checked for accuracy using another calibrated unit.

Experiments with rock cutting involved machining of cylindrical Georgia granite on a lathe using standard PDC inserts. Water was used as coolant and two conditions for

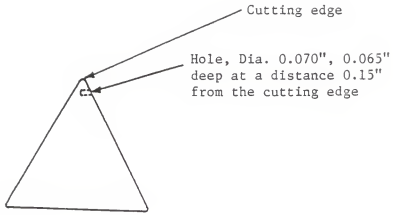

Figure 28 - Tungsten carbide tool for Experiment #1

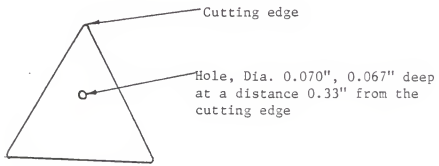

Figure 29 - Tungsten carbide tool for Experiment #2

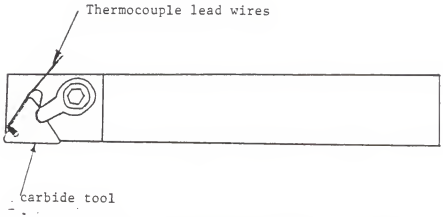

Figure 30 - Tool holder and thermocouple assembly for Experiment #1

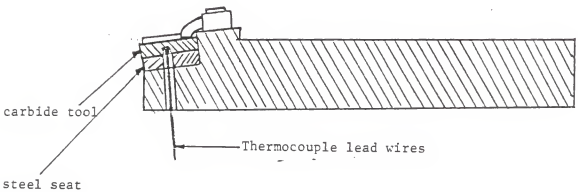

Figure 31 - Tool holder and thermocouple assembly for Experiment #2

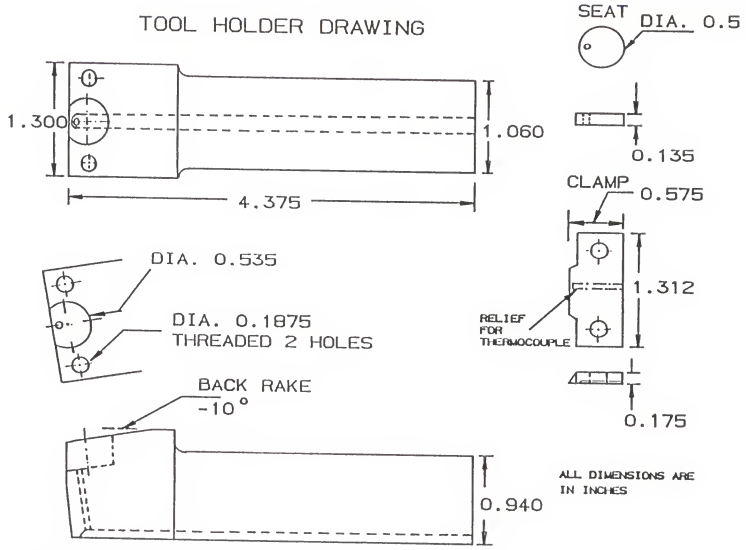

Figure 32 - Tool holder used for rock cutting experiments

cooling were employed. Sometimes, taper on the rock would result from tool wear. If taper was significant (more than 0.010" on diameter in 10" length), it was removed by machining with another tool.

The following experiments were performed (see Appendix B for data collected):

Experiment #3:

Feed: 0.020 ipr

Depth of Cut: 0.020"

RPM: variable. Effect of cutting speed being considered.

Cooling: by impinging a thin jet of water on the tool.

Distance of thermocouple from the cutting edge: Not considered.

Experiment #4:

Feed: 0.020 ipr

Depth of Cut: 0.020"

RPM: 290 - to maintain near constant cutting speed.

Cooling: by impinging a thin jet of water on the tool.

Distance of thermocouple from the cutting edge measured.

Experiment #5:

Feed: 0.020 ipr

Depth of Cut: 0.020"

RPM: 290 - to maintain near constant cutting speed.

Cooling: by wetting the rock from behind so that a uniform thin film of water was formed around it.

Distance of thermocouple from the cutting edge measured.

The diameter of the rock was measured using a micrometer before and after each run.

5.0 RESULTS AND DISCUSSION

5.1 Experiment #1 and #2 on Metal Cutting

The temperature curve (Figure 33) for Experiment #1 is far above that for Experiment #2 due to the following reasons:

1. The distance of the thermocouple from the cutting edge is less for #1, and

2. The depth of cut for #1 is twice that for #2.

Since the triangular insert was seated on a flat steel seat, it lost heat through the seat and into the tool holder. Temperatures at points farther away from the cutting edge would therefore be lower.

When the point considered was closer to the cutting edge, the temperature rise was steep. At a point farther from the cutting edge, due to the large amount of uniform cooling through the seat, the temperature rise was flat. This means that for any sensing required to be done for an adaptive control situation (changing machining parameters automatically based on temperature sensed), the temperature probe has to be as close to the cutting edge as possible. Only at a point closer to the cutting edge would the system be sensitive to changes in tool and work condition such as increased wear, hardness, etc.

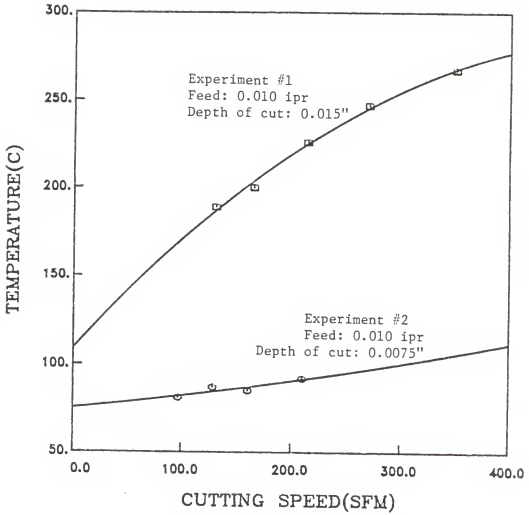

Figure 33 - Temperature plots for metal cutting experiments

5.2 Rock Cutting Experiments

5.2.1 Experiment #3:

In contrast to metal cutting, Figure 34 shows a steep rise in temperature with cutting speed. This can be attributed to the following:

1. In metal cutting, a large portion of the cutting heat is carried away by the chip and the workpiece. Rock being a much better insulator, most of the heat is absorbed by the tool.

2. As the cutting temperatures rise above 100 deg. C., the coolant begins to boil and turn to steam resulting in dry machining. This results in further rise in tool temperatures.

3. As the cutting temperatures rise, the diamond in the PDC insert begins to fail causing rapid wear. This further leads to increased wear land, increased heat generation due to friction at the rock tool interface, and therefore higher temperatures.

4. As the tool wears, the thermocouple progressively gets closer to the cutting edge and therefore encounters higher temperatures.

All of the above effects together cause a steep rise in temperatures.

Typically, in actual downhole drilling situation, all these effects would take place simultaneously. The stagnant water and slurry mix in the downhole would begin

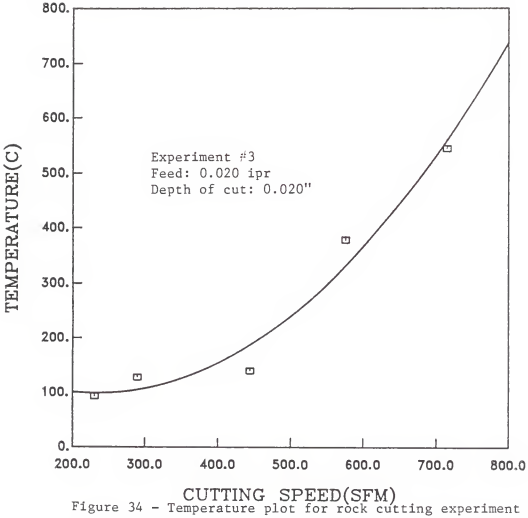

Figure 34 - Temperature plot for rock cutting experiment #3

to absorb heat and boil in the area of cutting. This may lead to dry drilling and rapid tool wear thereafter.

5.2.2 Experiment #4:

Figure 35 shows the plot of temperature measured when the cutting edge got closer to the thermocouple as the tool wore.

In this experiment, a thin jet of water hit the tool. This method of cooling was found ineffective both at lower and higher temperatures. This method triggered the following chain of events which resulted in rapid temperature rise and tool wear:

1. The thin jet did not have sufficient force to drive the rock dust away from the tool face.

2. More and more rock dust thus got accumulated on the tool face.

3. Water was unable to fully penetrate the dust accumulation and cooling became poor.

4. This made the temperatures to rise sharply.

5. As the temperatures rose, the little water which could reach the tool turned to steam, cooling completely failed and temperatures rose further.

6. As the cutting temperatures rose to the critical value of above 700 deg. C., rapid wear began to take place.

7. Again, as tool wear took place, the wear land and therefore heat generated by friction increased, resulting

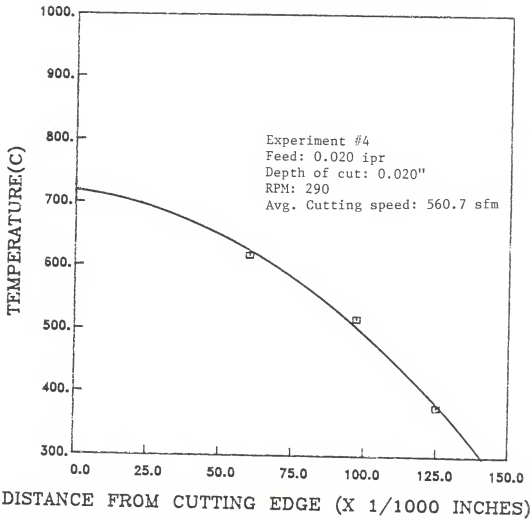

Figure 35 - Temperature Vs Distance plot for Experiment #4

in higher cutting temperatures.

All of the above result in temperatures nearing 400 deg. C. even at a distance of 0.125" from the cutting edge. Extrapolating the curve backwards indicates that temperature at the cutting edge is about 720 deg. C. which is just above the critical temperature for diamond.

5.2.3 Experiment #5:

Figure 36 represents the plot of temperature vs. distance. Here, cooling was done by wetting the rock from behind so that a uniform thin film of water was formed around it. The cooling by this method was found to be distinctly more effective than the one used in Experiment #4 at lower temperatures. In this case, the continuous film of water prevented the rock dust from accumulating on the tool. This allowed cooling of the tool to take place continuously. As can be seen from Figure 36, even at a distance as close as 0.060", the temperature measured was only between 100 and 200 deg. C. Because the temperatures were not rising, the tool in this experiment behaved exceedingly well wearing very slowly and therefore keeping temperatures down. As seen before, temperature and wear influence one another.

Since the tool would not wear, accelerated wear was done by reducing water flow and the experiment then conducted as before. Once the tool began to wear, the increased wear land and heat due to friction resulted in

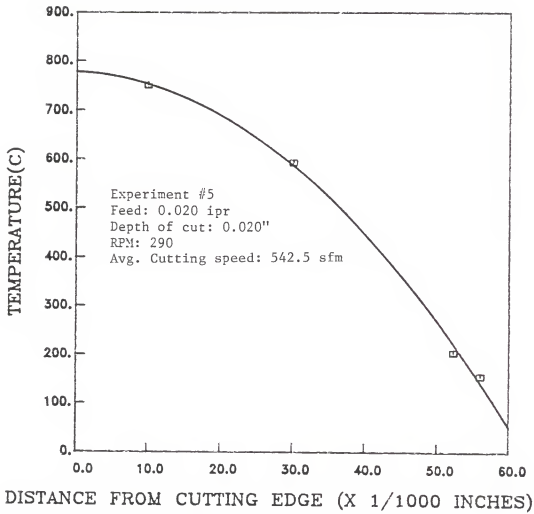

Figure 36 - Temperature Vs Distance plot for Experiment #5

higher temperatures, which in turn resulted in higher wear. As the temperatures increased, the coolant (water) began to boil and turn to steam resulting in dry machining. This implies that even if cooling is efficient at lower temperatures (which is the case when the tool is new), at higher temperatures it will always boil and evaporate resulting in dry machining, at least local to the cutting edge. Thus at higher temperature and wear situation, the effect of coolant will be negligible.

As before, extrapolation of the temperature curve indicates that temperature at the cutting edge for a wearing tool is in the range 750-800 deg. C.

6.0 CONCLUSIONS AND RECOMMENDATIONS

The experimental results from this study compare well with the theoretical model for the heat transfer and temperature distribution for PDC cutters developed by Prakash [1] and the experimental studies of Lee and Hibbs. The maximum temperature estimated at the cutting edge is in the region 720-800 deg. C. which compares to the theoretical results of Prakash. This is a significant result because it confirms the validity and accuracy of the thermal model.

Lavine [20] points out that when the workpiece surface temperature in grinding reaches a value slightly in excess of 100 deg. C., water-based fluid shows no advantage over dry grinding. Such an effect was more evident in rock cutting with cutting temperatures going much above 100 deg. C. The resulting visible dry machining was the cause of higher temperatures and wear.

In actual downhole condition, water based drilling fluid is pumped in with high velocity to act as coolant. Researchers have yet not been able to determine if this coolant velocity effectively serves all the cutting edges of the drill bit for cooling as well as chip removal. Heat dissipation at a cutting edge where the coolant velocity is insufficient to remove chips may be extremely slow causing film boiling of the coolant at the cutting edge. Thus even with water based fluid around, localized

dry rock drilling may occur in and around the cutting edge causing rapid wear.

J.G.Chow and P.K.Wright [21] conducted a study on metal cutting which in some respects is parallel to this study. It is interesting to note that just like the objective of this study, their objective was also to test an analytical model experimentally and estimate temperatures at tool/chip interface in a turning operation.

A set up for infrared radiation pyrometry has also been proposed for further experimentation in this study. The tool holder design is flexible and may be used either for thermocouple or IR temperature measurements.

This study also presents a methodology for temperature sensing for adaptive control in rock cutting by use of MWD (measurement while drilling). The feedback from the thermocouple or infrared device may be fed to a computer which would change rock cutting parameters such as RPM, depth of cut, etc to reduce tool temperatures and thereby prevent the diamond from reaching its critical temperature. This study coupled with that of Prakash therefore serves as a basis for designing control systems.

Additional experiments should be conducted to further test the effect of cooling beyond the boiling point of water. It is important to note that when the tool temperatures rise above 100 deg. C., the coolant would

quickly evaporate and the cutting would then be practically dry. This is a perfectly normal phenomemon and the experimenter should not worry about it. This means that a cut may begin normally but as the tool temperature rises, may turn to dry machining midway through the cut.

The lathe on which turning is done should be equipped with a speed controller to enable small changes in RPM to keep the cutting speed constant. This would reduce the variability between each run, and repeatability could then be attempted.

Experiments should be conducted at different constant cutting speeds. This will be useful in correlating critical temperature and cutting speed as done by Prakash.

REFERENCES

1. Prakash, V., Finite Element Method for Temperature Distribution in Synthetic Diamond Cutters during Orthogonal Rock Cutting, Dissertation, Kansas State University, 1986.

2. Lee, M. and L. E. Hibbs, Jr., Role of Deformation Twin Bands in the Wear Processes of Polycrystalline Diamond Tools, ASME, Wear of Materials, Ed. K. C. Ludema, W.A. Glaeser, S. K. Rhee, 1979, p. 485.

3. Quinn, T. J., Temperature, Academic Press, 1983.

4. Pollock, D. D., The Theory and Properties of Thermocouple Elements, American Society for Testing and Materials, 1971.

5. Benedict, R. P., Fundamentals of Temperature, Pressure, and Flow measurements, John Wiley & Sons, 1984.

6. Kinzie, P. A., Thermocouple Temperature Measurement, John Wiley & Sons, 1973.

7. Trent, E. M., Metal Cutting, Butterworths, 1978.

8. Shaw, M. C., Metal Cutting Principles, Oxford University Press, 1986.

9. Boothroyd, G., Temperatures in Orthogonal Metal Cutting, Proc Instn Mech Engrs, Vol 177, No 29, 1963, p. 789.

10. Wright, P. K., Applications of the Experimental Methods Used to Determine Temperature Gradients in Cutting Tools, Austrlian Conference on Manufacturing Engineering, 17-19 August 1977, The Institution of Engineers, Australia, National Conference Publication No. 77/7, p.145.

11. Triemel, J. and Panhorst, H. J., Heat generation and temperature measurement in diamond machining operations, Industrial Diamond Review, March 1973, p. 95.

12. Barrow, G., A Review of Experimental and Theoretical Techniques for Assessing Cutting Temperatures, Annals of the C. I. R. P., Vol. 22/2, 1973, p. 203.

13. Kazuaki, I., Toshimichi, M., Koichi, O., A study of Cutting Temperature in Ultra-High Precision Diamond Cutting of Copper (OFC), SME Manufacturing Tech.

Review, Vol. 2, 15th NAMRC, 1987, p. 510.

14. Panhorst, J., Triemel, J., Temperature determination in grinding - measurements and model tests with diamond and corundum single particle tools, Industrial Diamond Review, September 1976, p. 320.

15. Harris, A., Hastings, W. F., and Mathew, P., The Experimental Measurement of Cutting Temperature, International Conference on Manufacturing Engineering, August 1980, The Institution of Engineers, Australia, National Conference Publication No 80/5, p. 30.

16. Kops, L., and Shaw, M. C., Application of Infrared radiation Measurements in Grinding Studies, SME Manufacturing Engineering Transactions, 11th NAMRC, 1983, p. 390.

17. Ueda, T., Hosokawa, A., and Yamamoto, A., Studies on Temperature of Abrasive Grains in Grinding - Application of Infrared Radiation Pyrometer, Journal of Engineering for Industry, ASME Trans., May 1985, Vol. 107, p. 127.

18. Bernard, B., abc's of Infrared, Howard W. Sams & Co., Inc., 1970.

19. Ueda, T., Hosokawa, A., and Yamamoto, A., Measurement of Grinding Temperature Using Infrared Radiation Pyrometer With Optical Fiber, Journal of Engineering for Industry, ASME Trans., November 1986, Vol. 108, p. 247.

20. Lavine, A. S., A Simple Model for Convective Cooling During the Grinding Process, Journal of Engineering for Industry, ASME Trans., February 1988, Vol. 110, p. 1.

21. Chow, J. G., Wright, P. K., On-Line Estimation of Tool/Chip Interface Temperatures for a Turning Operation, Journal of Engineering for Industry, ASME Trans., February 1988, Vol. 110, p. 56.

CHROMEL vs. ALUMEL THERMOCOUPLE

Degrees Celsius — Reference Junction 0° C.

°C	0	1	2	3	4	5	6	7	8	9
					Millivolts					
0	0.00	0.04	0.08	0.12	0.16	0.20	0.24	0.28	0.32	0.36
10	0.40	0.44	0.48	0.52	0.56	0.60	0.64	0.68	0.72	0.76
20	0.80	0.84	0.88	0.92	0.96	1.00	1.04	1.08	1.12	1.16
30	1.20	1.24	1.28	1.32	1.36	1.40	1.44	1.49	1.53	1.57
40	1.61	1.65	1.69	1.73	1.77	1.81	1.85	1.90	1.94	1.98
50	2.02	2.06	2.10	2.14	2.18	2.23	2.27	2.31	2.35	2.39
60	2.43	2.47	2.51	2.56	2.60	2.64	2.68	2.72	2.76	2.80
70	2.85	2.89	2.93	2.97	3.01	3.05	3.10	3.14	3.18	3.22
80	3.26	3.30	3.35	3.39	3.43	3.47	3.51	3.56	3.60	3.64
90	3.68	3.72	3.76	3.81	3.85	3.89	3.93	3.97	4.01	4.06
100	4.10	4.14	4.18	4.22	4.26	4.31	4.35	4.39	4.43	4.47
110	4.51	4.55	4.60	4.64	4.68	4.72	4.76	4.80	4.84	4.88
120	4.92	4.96	5.01	5.05	5.09	5.13	5.17	5.21	5.25	5.29
130	5.33	5.37	5.41	5.45	5.49	5.53	5.57	5.61	5.65	5.69
140	5.73	5.77	5.81	5.85	5.89	5.93	5.97	6.01	6.05	6.09
150	6.13	6.17	6.21	6.25	6.29	6.33	6.37	6.41	6.45	6.49
160	6.53	6.57	6.61	6.65	6.69	6.73	6.77	6.81	6.85	6.89
170	6.93	6.97	7.01	7.05	7.09	7.13	7.17	7.21	7.25	7.29
180	7.33	7.37	7.41	7.45	7.49	7.53	7.57	7.61	7.65	7.69
190	7.73	7.77	7.81	7.85	7.89	7.93	7.97	8.01	8.05	8.09
200	8.13	8.17	8.21	8.25	8.29	8.33	8.37	8.41	8.46	8.50
210	8.54	8.58	8.62	8.66	8.70	8.74	8.78	8.82	8.86	8.90
220	8.94	8.98	9.02	9.06	9.10	9.14	9.18	9.22	9.26	9.30
230	9.34	9.38	9.42	9.46	9.50	9.54	9.59	9.63	9.67	9.71
240	9.75	9.79	9.83	9.87	9.91	9.95	9.99	10.03	10.07	10.11
250	10.16	10.20	10.24	10.28	10.32	10.36	10.40	10.44	10.48	10.52
260	10.57	10.61	10.65	10.69	10.73	10.77	10.81	10.85	10.89	10.93
270	10.98	11.02	11.06	11.10	11.14	11.18	11.22	11.26	11.30	11.34
280	11.39	11.43	11.47	11.51	11.55	11.59	11.63	11.67	11.72	11.76
290	11.80	11.84	11.88	11.92	11.96	12.01	12.05	12.09	12.13	12.17
300	12.21	12.25	12.29	12.34	12.38	12.42	12.46	12.50	12.54	12.58
310	12.63	12.67	12.71	12.75	12.79	12.83	12.88	12.92	12.96	13.00
320	13.04	13.08	13.12	13.17	13.21	13.25	13.29	13.33	13.37	13.42
330	13.46	13.50	13.54	13.58	13.62	13.67	13.71	13.75	13.79	13.83
340	13.88	13.92	13.96	14.00	14.04	14.09	14.13	14.17	14.21	14.25
350	14.29	14.34	14.38	14.42	14.46	14.50	14.55	14.59	14.63	14.67
360	14.71	14.76	14.80	14.84	14.88	14.92	14.97	15.01	15.05	15.09
370	15.13	15.18	15.22	15.26	15.30	15.34	15.39	15.43	15.47	15.51
380	15.55	15.60	15.64	15.68	15.72	15.78	15.81	15.85	15.89	15.93
390	15.98	16.02	16.06	16.10	16.14	16.18	16.23	16.27	16.31	16.36
400	16.40	16.44	16.48	16.52	16.57	16.61	16.65	16.69	16.74	16.78
410	16.82	16.86	16.91	16.95	16.99	17.03	17.07	17.12	17.16	17.20
420	17.24	17.29	17.33	17.37	17.41	17.46	17.50	17.54	17.58	17.62
430	17.67	17.71	17.75	17.79	17.84	17.88	17.92	17.96	18.01	18.05
440	18.09	18.13	18.17	18.22	18.26	18.30	18.34	18.39	18.43	18.47
450	18.51	18.56	18.60	18.64	18.68	18.73	18.77	18.81	18.85	18.90
460	18.94	18.98	19.02	19.07	19.11	19.15	19.19	19.24	19.28	19.32
470	19.36	19.41	19.45	19.49	19.54	19.58	19.62	19.66	19.71	19.75
480	19.79	19.84	19.88	19.92	19.96	20.01	20.05	20.09	20.13	20.18
490	20.22	20.26	20.31	20.35	20.39	20.43	20.48	20.52	20.56	20.60
500	20.65	20.69	20.73	20.77	20.82	20.86	20.90	20.94	20.99	21.03
510	21.07	21.11	21.16	21.20	21.24	21.28	21.32	21.37	21.41	21.45
520	21.50	21.54	21.58	21.63	21.67	21.71	21.75	21.80	21.84	21.88
530	21.92	21.97	22.01	22.05	22.09	22.14	22.18	22.22	22.26	22.31
540	22.35	22.39	22.43	22.48	22.52	22.56	22.61	22.65	22.69	22.73
550	22.78	22.82	22.86	22.90	22.95	22.99	23.03	23.07	23.12	23.16
560	23.20	23.25	23.29	23.33	23.38	23.42	23.46	23.50	23.54	23.59
570	23.63	23.67	23.72	23.76	23.80	23.84	23.89	23.93	23.97	24.01
580	24.06	24.10	24.14	24.18	24.23	24.27	24.31	24.36	24.40	24.44
590	24.49	24.53	24.57	24.61	24.65	24.70	24.74	24.78	24.83	24.87

CHROMEL vs. ALUMEL THERMOCOUPLE

Degrees Celsius — Reference Junction 0° C.

°C	0	1	2	3	4	5	6	7	8	9
					Millivolts					
600	24.91	24.95	25.00	25.04	25.08	25.12	25.17	25.21	25.25	25.29
610	25.34	25.38	25.42	25.47	25.51	25.55	25.59	25.64	25.68	25.72
620	25.76	25.81	25.85	25.89	25.93	25.98	26.02	26.06	26.10	26.15
630	26.19	26.23	26.27	26.32	26.36	26.40	26.44	26.48	26.53	26.57
640	26.61	26.65	26.70	26.74	26.78	26.82	26.86	26.91	26.95	26.99
650	27.03	27.07	27.12	27.16	27.20	27.24	27.28	27.33	27.37	27.41
660	27.45	27.49	27.54	27.58	27.62	27.66	27.71	27.75	27.79	27.83
670	27.87	27.92	27.96	28.00	28.04	28.08	28.13	28.17	28.21	28.25
680	28.29	28.34	28.38	28.42	28.46	28.50	28.55	28.59	28.63	28.67
690	28.72	28.76	28.80	28.84	28.88	28.93	28.97	29.01	29.05	29.10
700	29.14	29.18	29.22	29.26	29.30	29.35	29.39	29.43	29.47	29.52
710	29.56	29.60	29.64	29.68	29.72	29.77	29.81	29.85	29.89	29.93
720	29.97	30.02	30.06	30.10	30.14	30.18	30.23	30.27	30.31	30.35
730	30.39	30.44	30.48	30.52	30.56	30.60	30.65	30.69	30.73	30.77
740	30.81	30.85	30.90	30.94	30.98	31.02	31.06	31.10	31.15	31.19
750	31.23	31.27	31.31	31.35	31.40	31.44	31.48	31.52	31.56	31.60
760	31.65	31.69	31.73	31.77	31.81	31.85	31.90	31.94	31.98	32.02
770	32.06	32.10	32.15	32.19	32.23	32.27	32.31	32.35	32.39	32.43
780	32.48	32.52	32.56	32.60	32.64	32.68	32.72	32.76	32.81	32.85
790	32.89	32.93	32.97	33.01	33.05	33.09	33.13	33.18	33.22	33.26
800	33.30	33.34	33.38	33.42	33.46	33.50	33.54	33.59	33.63	33.67
810	33.71	33.75	33.79	33.83	33.87	33.91	33.95	33.99	34.04	34.08
820	34.12	34.16	34.20	34.24	34.28	34.32	34.36	34.40	34.44	34.48
830	34.53	34.57	34.61	34.65	34.69	34.73	34.77	34.61	34.65	34.59
840	34.93	34.97	35.02	35.06	35.10	35.14	35.18	35.22	35.26	35.30
850	35.34	35.38	35.42	35.46	35.50	35.54	35.58	35.63	35.67	35.71
860	35.75	35.79	35.83	35.87	35.91	35.95	35.99	36.03	36.07	36.11
870	36.15	36.19	36.23	36.27	36.31	36.35	36.39	36.43	36.47	36.51
880	36.55	36.59	36.63	36.67	36.72	36.76	36.60	36.84	36.88	36.92
890	36.96	37.00	37.04	37.08	37.12	37.16	37.20	37.24	37.28	37.32
900	37.36	37.40	37.44	37.48	37.52	37.56	37.60	37.64	37.68	37.72
910	37.76	37.80	37.84	37.88	37.92	37.96	38.00	38.04	38.08	38.12
920	38.16	38.20	38.24	38.28	38.32	38.36	38.40	38.44	38.48	38.52
930	38.56	38.60	38.64	38.68	38.72	38.76	38.80	38.84	38.88	38.92
940	38.95	38.99	39.03	39.07	39.11	39.15	39.19	39.23	39.27	39.31
950	39.35	39.39	39.43	39.47	39.51	39.55	39.59	39.63	39.67	39.71
960	39.75	39.79	39.83	39.86	39.90	39.94	39.98	40.02	40.06	40.10
970	40.14	40.18	40.22	40.26	40.30	40.34	40.38	40.41	40.45	40.49
980	40.53	40.57	40.61	40.65	40.69	40.73	40.77	40.81	40.85	40.89
990	40.92	40.96	41.00	41.04	41.08	41.12	41.16	41.20	41.24	41.28
1000	41.31	41.35	41.39	41.43	41.47	41.51	41.55	41.59	41.63	41.67
1010	41.70	41.74	41.78	41.82	41.86	41.90	41.94	41.98	42.02	42.05
1020	42.09	42.13	42.17	42.21	42.25	42.29	42.33	42.36	42.40	42.44
1030	42.48	42.52	42.56	42.60	42.63	42.67	42.71	42.75	42.79	42.83
1040	42.87	42.90	42.94	42.98	43.02	43.06	43.10	43.14	43.17	43.21
1050	43.25	43.29	43.33	43.37	43.41	43.44	43.48	43.52	43.56	43.60
1060	43.63	43.67	43.71	43.75	43.79	43.83	43.87	43.90	43.94	43.98
1070	44.02	44.06	44.10	44.13	44.17	44.21	44.25	44.29	44.33	44.36
1080	44.40	44.44	44.48	44.52	44.55	44.59	44.63	44.67	44.71	44.74
1090	44.78	44.82	44.86	44.90	44.93	44.97	45.01	45.05	45.09	45.12
1100	45.16	45.20	45.24	45.27	45.31	45.35	45.39	45.43	45.48	45.50
1110	45.54	45.58	45.62	45.65	45.69	45.73	45.77	45.80	45.84	45.88
1120	45.92	45.96	45.99	46.03	46.07	46.11	46.14	46.18	46.22	46.26
1130	46.29	46.33	46.37	46.41	46.44	46.48	46.52	46.56	46.59	46.63
1140	46.67	46.70	46.74	46.78	46.82	46.85	46.89	46.93	46.97	47.00
1150	47.04	47.08	47.12	47.15	47.19	47.23	47.26	47.30	47.34	47.38
1160	47.41	47.45	47.49	47.52	47.56	47.60	47.63	47.67	47.71	47.75
1170	47.78	47.82	47.86	47.89	47.93	47.97	48.00	48.04	48.08	48.12
1180	48.15	48.19	48.23	48.26	48.30	48.34	48.37	48.41	48.45	48.48
1190	48.52	48.56	48.59	48.63	48.67	48.70	48.74	48.78	48.81	48.85

CHROMEL vs. ALUMEL THERMOCOUPLE

Degrees Celsius — Reference Junction 0° C.

°C	0	1	2	3	4	5	6	7	8	9
					Millivolts					
1200	48.89	48.92	48.96	49.00	49.03	49.07	49.11	49.14	49.18	49.22
1210	49.25	49.29	49.32	49.36	49.40	49.43	49.47	49.51	49.54	49.58
1220	49.62	49.65	49.69	49.72	49.76	49.80	49.83	49.87	49.90	49.94
1230	49.98	50.01	50.05	50.08	50.12	50.16	50.19	50.23	50.26	50.30
1240	50.34	50.37	50.41	50.44	50.48	50.52	50.55	50.59	50.62	50.66
1250	50.69	50.73	50.77	50.80	50.84	50.87	50.91	50.94	50.98	51.02
1260	51.05	51.09	51.12	51.16	51.19	51.23	51.27	51.30	51.34	51.37
1270	51.41	51.44	51.48	51.51	51.55	51.55	51.62	51.66	51.69	51.73
1280	51.76	51.80	51.83	51.87	51.90	51.94	51.97	52.01	52.04	52.08
1290	52.11	52.15	52.18	52.22	52.25	52.29	52.32	52.36	52.39	52.43
1300	52.46	52.50	52.53	52.57	52.60	52.64	52.67	52.71	52.74	52.78
1310	52.81	52.85	52.88	52.92	52.95	52.99	53.02	53.06	53.09	53.13
1320	53.16	53.20	53.23	53.27	53.30	53.34	53.37	53.41	53.44	53.47
1330	53.51	53.54	53.58	53.61	53.65	53.68	53.72	53.75	53.79	53.82
1340	53.85	53.89	53.92	53.96	53.99	54.03	54.06	54.10	54.13	54.16
1350	54.20	54.23	54.27	54.30	54.34	54.37	54.40	54.44	54.47	54.51
1360	54.54	54.57	54.61	54.64	54.68	54.71	54.74	54.78	54.81	54.85
1370	54.88	54.91								

CHROMEL vs. ALUMEL THERMOCOUPLE

Degrees Fahrenheit — Reference Junction 32° F.

°F	0	1	2	3	4	5	6	7	8	9
					Millivolts					
0	-0.68	-0.66	-0.64	-0.62	-0.60	-0.58	-0.56	-0.54	-0.52	-0.49
10	-0.47	-0.45	-0.43	-0.41	-0.39	-0.37	-0.34	-0.32	-0.30	-0.28
20	-0.26	-0.24	-0.22	-0.19	-0.17	-0.15	-0.13	-0.11	-0.09	-0.07
30	-0.04	-0.02	0.00	0.02	0.04	0.07	0.09	0.11	0.13	0.15
40	0.18	0.20	0.22	0.24	0.26	0.29	0.31	0.33	0.35	0.37
50	0.40	0.42	0.44	0.46	0.48	0.51	0.53	0.55	0.57	0.60
60	0.62	0.64	0.66	0.68	0.71	0.73	0.75	0.77	0.80	0.82
70	0.84	0.86	0.88	0.91	0.93	0.95	0.97	1.00	1.02	1.04
80	1.06	1.09	1.11	1.13	1.15	1.18	1.20	1.22	1.24	1.27
90	1.29	1.31	1.33	1.36	1.38	1.40	1.43	1.45	1.47	1.49
100	1.52	1.54	1.56	1.58	1.61	1.63	1.65	1.68	1.70	1.72
110	1.74	1.77	1.79	1.81	1.84	1.86	1.88	1.90	1.93	1.95
120	1.97	2.00	2.02	2.04	2.06	2.09	2.11	2.13	2.16	2.18
130	2.20	2.23	2.25	2.27	2.29	2.32	2.34	2.36	2.39	2.41
140	2.43	2.46	2.48	2.50	2.52	2.55	2.57	2.59	2.62	2.64
150	2.66	2.69	2.71	2.73	2.75	2.78	2.80	2.82	2.85	2.87
160	2.89	2.92	2.94	2.96	2.98	3.01	3.03	3.05	3.08	3.10
170	3.12	3.15	3.17	3.19	3.22	3.24	3.26	3.29	3.31	3.33
180	3.36	3.38	3.40	3.43	3.45	3.47	3.49	3.52	3.54	3.56
190	3.59	3.61	3.63	3.66	3.68	3.70	3.73	3.75	3.77	3.80
200	3.82	3.84	3.87	3.89	3.91	3.94	3.96	3.98	4.01	4.03
210	4.05	4.08	4.10	4.12	4.15	4.17	4.19	4.21	4.24	4.26
220	4.28	4.31	4.33	4.35	4.38	4.40	4.42	4.44	4.47	4.49
230	4.51	4.54	4.56	4.58	4.61	4.63	4.65	4.67	4.70	4.72
240	4.74	4.77	4.79	4.81	4.83	4.86	4.88	4.90	4.92	4.95
250	4.97	4.99	5.02	5.04	5.06	5.08	5.11	5.13	5.15	5.17
260	5.20	5.22	5.24	5.26	5.29	5.31	5.33	5.35	5.38	5.40
270	5.42	5.44	5.47	5.49	5.51	5.53	5.56	5.58	5.60	5.62
280	5.65	5.67	5.69	5.71	5.73	5.76	5.78	5.80	5.82	5.85
290	5.87	5.89	5.91	5.93	5.96	5.98	6.00	6.02	6.05	6.07
300	6.09	6.11	6.13	6.16	6.18	6.20	6.22	6.25	6.27	6.29
310	6.31	6.33	6.36	6.38	6.40	6.42	6.45	6.47	6.49	6.51
320	6.53	6.56	6.58	6.60	6.62	6.65	6.67	6.69	6.71	6.73
330	6.76	6.78	6.80	6.82	6.84	6.87	6.89	6.91	6.93	6.96
340	6.98	7.00	7.02	7.04	7.07	7.09	7.11	7.13	7.15	7.18
350	7.20	7.22	7.24	7.26	7.29	7.31	7.33	7.35	7.38	7.40
360	7.42	7.44	7.46	7.49	7.51	7.53	7.55	7.58	7.60	7.62
370	7.64	7.68	7.69	7.71	7.73	7.75	7.78	7.80	7.82	7.84
380	7.87	7.89	7.91	7.93	7.95	7.98	8.00	8.02	8.04	8.07
390	8.09	8.11	8.13	8.18	8.18	8.20	8.22	8.24	8.27	8.29
400	8.31	8.33	8.36	8.38	8.40	8.42	8.45	8.47	8.49	8.51
410	8.54	8.56	8.58	8.60	8.62	8.65	8.67	8.69	8.71	8.74
420	8.76	8.78	8.80	8.82	8.85	8.87	8.89	8.91	8.94	8.96
430	8.98	9.00	9.03	9.05	9.07	9.09	9.12	9.14	9.16	9.18
440	9.21	9.23	9.25	9.27	9.30	9.32	9.34	9.36	9.39	9.41
450	9.43	9.45	9.48	9.50	9.52	9.54	9.57	9.59	9.61	9.63
460	9.66	9.68	9.70	9.73	9.75	9.77	9.79	9.82	9.84	9.86
470	9.88	9.91	9.93	9.95	9.97	10.00	10.02	10.04	10.06	10.09
480	10.11	10.13	10.16	10.18	10.20	10.22	10.25	10.27	10.29	10.31
490	10.34	10.36	10.38	10.40	10.43	10.45	10.47	10.50	10.52	10.54
500	10.57	10.59	10.61	10.63	10.66	10.68	10.70	10.72	10.75	10.77
510	10.79	10.82	10.84	10.86	10.88	10.91	10.93	10.95	10.98	11.00
520	11.02	11.04	11.07	11.09	11.11	11.13	11.18	11.18	11.20	11.23
530	11.25	11.27	11.29	11.32	11.34	11.36	11.39	11.41	11.43	11.45
540	11.48	11.50	11.52	11.55	11.57	11.59	11.61	11.64	11.68	11.68
550	11.71	11.73	11.75	11.78	11.80	11.82	11.84	11.87	11.89	11.91
560	11.94	11.96	11.98	12.01	12.03	12.05	12.07	12.10	12.12	12.14
570	12.17	12.19	12.21	12.24	12.26	12.28	12.30	12.33	12.35	12.37
580	12.40	12.42	12.44	12.47	12.49	12.51	12.53	12.56	12.58	12.60
590	12.63	12.65	12.67	12.70	12.72	12.74	12.78	12.79	12.81	12.83

CHROMEL vs. ALUMEL THERMOCOUPLE

Degrees Fahrenheit — Reference Junction 32° F.

°F	0	1	2	3	4	5	6	7	8	9
					Millivolts					
600	12.86	12.88	12.90	12.93	12.95	12.97	13.00	13.02	13.04	13.06
610	13.09	13.11	13.13	13.16	13.18	13.20	13.23	13.25	13.27	13.30
620	13.32	13.34	13.36	13.39	13.41	13.44	13.46	13.48	13.50	13.53
630	13.55	13.57	13.60	13.62	13.64	13.67	13.69	13.71	13.74	13.76
640	13.78	13.81	13.83	13.85	13.88	13.90	13.92	13.95	13.97	13.99
650	14.02	14.04	14.06	14.09	14.11	14.13	14.15	14.18	14.20	14.22
660	14.25	14.27	14.29	14.32	14.34	14.36	14.39	14.41	14.43	14.46
670	14.48	14.50	14.53	14.55	14.57	14.60	14.62	14.64	14.67	14.69
680	14.71	14.74	14.76	14.78	14.81	14.83	14.85	14.88	14.90	14.92
690	14.95	14.97	14.99	15.02	15.04	15.06	15.09	15.11	15.13	15.16
700	15.18	15.20	15.23	15.25	15.27	15.30	15.32	15.34	15.37	15.39
710	15.41	15.44	15.48	15.48	15.51	15.53	15.55	15.58	15.60	15.62
720	15.65	15.67	15.69	15.72	15.74	15.76	15.79	15.81	15.83	15.86
730	15.88	15.90	15.93	15.95	15.98	16.00	16.02	16.05	16.07	16.09
740	16.12	16.14	16.16	16.19	16.21	16.23	16.26	16.28	16.30	16.33
750	16.35	16.37	16.40	16.42	16.45	16.47	16.49	16.52	16.54	16.56
760	16.59	16.61	16.63	16.66	16.68	16.70	16.73	16.75	16.77	16.80
770	16.82	16.84	16.87	16.89	16.92	16.94	16.96	16.99	17.01	17.03
780	17.06	17.08	17.10	17.13	17.15	17.17	17.20	17.22	17.24	17.27
790	17.29	17.31	17.34	17.36	17.39	17.41	17.43	17.46	17.48	17.50
800	17.53	17.55	17.57	17.60	17.62	17.64	17.67	17.69	17.71	17.74
810	17.76	17.78	17.81	17.83	17.86	17.88	17.90	17.93	17.95	17.97
820	18.00	18.02	18.04	18.07	18.09	18.11	18.14	18.16	18.18	18.21
830	18.23	18.25	18.28	18.30	18.33	18.35	18.37	18.40	18.42	18.44
840	18.47	18.49	18.51	18.54	18.56	18.58	18.61	18.63	18.65	18.68
850	18.70	18.73	18.75	18.77	18.80	18.82	18.84	18.87	18.89	18.91
860	18.94	18.96	18.99	19.01	19.03	19.06	19.08	19.10	19.13	19.15
870	19.18	19.20	19.22	19.25	19.27	19.29	19.32	19.34	19.36	19.39
880	19.41	19.44	19.46	19.48	19.51	19.53	19.55	19.58	19.60	19.63
890	19.65	19.67	19.70	19.72	19.75	19.77	19.79	19.82	19.84	19.86
900	19.89	19.91	19.94	19.96	19.98	20.01	20.03	20.05	20.08	20.10
910	20.13	20.15	20.17	20.20	20.22	20.24	20.27	20.29	20.32	20.34
920	20.36	20.39	20.41	20.43	20.46	20.48	20.50	20.53	20.55	20.58
930	20.60	20.62	20.65	20.67	20.69	20.72	20.74	20.76	20.79	20.81
940	20.84	20.86	20.88	20.91	20.93	20.95	20.98	21.00	21.03	21.05
950	21.07	21.10	21.12	21.14	21.17	21.19	21.21	21.24	21.26	21.28
960	21.31	21.33	21.36	21.38	21.40	21.43	21.45	21.47	21.50	21.52
970	21.54	21.57	21.59	21.62	21.64	21.66	21.69	21.71	21.73	21.76
980	21.78	21.81	21.83	21.85	21.88	21.90	21.92	21.95	21.97	21.99
990	22.02	22.04	22.07	22.09	22.11	22.14	22.16	22.18	22.21	22.23
1000	22.26	22.28	22.30	22.33	22.35	22.37	22.40	22.42	22.44	22.47
1010	22.49	22.52	22.54	22.56	22.59	22.61	22.63	22.66	22.68	22.71
1020	22.73	22.75	22.78	22.80	22.82	22.85	22.87	22.90	22.92	22.94
1030	22.97	22.99	23.01	23.04	23.06	23.08	23.11	23.13	23.16	23.18
1040	23.20	23.23	23.25	23.27	23.30	23.32	23.35	23.37	23.39	23.42
1050	23.44	23.48	23.49	23.51	23.54	23.56	23.58	23.81	23.63	23.65
1060	23.68	23.70	23.72	23.75	23.77	23.80	23.82	23.84	23.87	23.89
1070	23.91	23.94	23.96	23.99	24.01	24.03	24.06	24.08	24.10	24.13
1080	24.15	24.18	24.20	24.22	24.25	24.27	24.29	24.32	24.34	24.36
1090	24.39	24.41	24.44	24.46	24.49	24.51	24.53	24.55	24.58	24.80
1100	24.63	24.65	24.67	24.70	24.72	24.74	24.77	24.79	24.82	24.84
1110	24.86	24.89	24.91	24.93	24.96	24.98	25.01	25.03	25.05	25.08
1120	25.10	25.12	25.15	25.17	25.20	25.22	25.24	25.27	25.29	25.31
1130	25.34	25.36	25.38	25.41	25.43	25.46	25.48	25.50	25.53	25.55
1140	25.57	25.60	25.62	25.65	25.67	25.69	25.72	25.74	25.78	25.79
1150	25.81	25.83	25.88	25.88	25.91	25.93	25.95	25.98	28.00	26.02
1160	26.05	26.07	28.09	28.12	28.14	26.16	28.19	26.21	26.24	26.26
1170	26.28	26.31	26.33	28.35	26.38	26.40	26.42	26.45	28.47	26.49
1180	26.52	26.54	28.56	26.59	26.81	26.63	26.66	26.68	28.70	28.73
1190	26.75	26.77	26.80	26.82	26.85	26.87	26.89	26.91	26.94	26.96

CHROMEL vs. ALUMEL THERMOCOUPLE

Degrees Fahrenheit — Reference Junction 32° F.

°F	0	1	2	3	4	5	6	7	8	9
					Millivolts					
1200	26.98	27.01	27.03	27.06	27.08	27.10	27.12	27.15	27.17	27.20
1210	27.22	27.24	27.27	27.29	27.31	27.34	27.36	27.38	27.40	27.43
1220	27.45	27.48	27.50	27.52	27.55	27.57	27.59	27.62	27.64	27.66
1230	27.69	27.71	27.73	27.76	27.78	27.80	27.83	27.85	27.87	27.90
1240	27.92	27.94	27.97	27.99	28.01	28.04	28.06	28.08	28.11	28.13
1250	28.15	28.18	28.20	28.22	28.25	28.27	28.29	28.32	28.34	28.37
1260	28.39	28.41	28.44	28.46	28.48	28.50	28.53	28.55	28.58	28.60
1270	28.62	28.65	28.67	28.69	28.72	28.74	28.76	28.79	28.81	28.83
1280	28.86	28.88	28.90	28.93	28.95	28.97	29.00	29.02	29.04	29.07
1290	29.09	29.11	29.14	29.16	29.18	29.21	29.23	29.25	29.28	29.30
1300	29.32	29.35	29.37	29.39	29.42	29.44	29.46	29.49	29.51	29.53
1310	29.56	29.58	29.60	29.63	29.65	29.67	29.70	29.72	29.74	29.77
1320	29.79	29.81	29.84	29.86	29.88	29.91	29.93	29.95	29.97	30.00
1330	30.02	30.05	30.07	30.09	30.11	30.14	30.16	30.18	30.21	30.23
1340	30.25	30.28	30.30	30.32	30.35	30.37	30.39	30.42	30.44	30.46
1350	30.49	30.51	30.53	30.56	30.58	30.60	30.63	30.65	30.67	30.70
1360	30.72	30.74	30.77	30.79	30.81	30.83	30.86	30.88	30.90	30.93
1370	30.95	30.97	31.00	31.02	31.04	31.07	31.09	31.11	31.14	31.16
1380	31.18	31.21	31.23	31.25	31.28	31.30	31.32	31.34	31.37	31.39
1390	31.42	31.44	31.48	31.48	31.51	31.53	31.55	31.58	31.60	31.62
1400	31.65	31.67	31.69	31.72	31.74	31.76	31.78	31.81	31.83	31.85
1410	31.88	31.90	31.92	31.95	31.97	31.99	32.02	32.04	32.06	32.08
1420	32.11	32.13	32.15	32.18	32.20	32.22	32.25	32.27	32.29	32.31
1430	32.34	32.36	32.38	32.41	32.43	32.45	32.48	32.50	32.52	32.54
1440	32.57	32.59	32.61	32.64	32.66	32.68	32.70	32.73	32.75	32.77
1450	32.80	32.82	32.84	32.86	32.89	32.91	32.93	32.98	32.98	33.00
1460	33.02	33.05	33.07	33.09	33.12	33.14	33.16	33.18	33.21	33.23
1470	33.25	33.28	33.30	33.32	33.34	33.37	33.39	33.41	33.43	33.46
1480	33.48	33.50	33.53	33.55	33.57	33.59	33.62	33.64	33.66	33.69
1490	33.71	33.73	33.75	33.78	33.80	33.82	33.84	33.87	33.89	33.91
1500	33.93	33.96	33.98	34.00	34.03	34.05	34.07	34.09	34.12	34.14
1510	34.16	34.18	34.21	34.23	34.25	34.28	34.30	34.32	34.34	34.37
1520	34.39	34.41	34.43	34.46	34.48	34.50	34.53	34.55	34.57	34.59
1530	34.62	34.64	34.66	34.68	34.71	34.73	34.75	34.77	34.80	34.82
1540	34.84	34.87	34.89	34.91	34.93	34.96	34.98	35.00	35.02	35.05
1550	35.07	35.09	35.11	35.14	35.16	35.18	35.21	35.23	35.25	35.27
1560	35.29	35.32	35.34	35.36	35.39	35.41	35.43	35.45	35.48	35.50
1570	35.52	35.54	35.57	35.59	35.61	35.63	35.66	35.68	35.70	35.72
1580	35.75	35.77	35.79	35.81	35.84	35.86	35.88	35.90	35.93	35.95
1590	35.97	35.99	36.02	36.04	36.06	36.08	36.11	36.13	36.15	36.17
1600	36.19	36.22	36.24	36.26	36.29	36.31	36.33	36.35	36.37	36.40
1610	36.42	36.44	36.46	36.49	36.51	36.53	36.55	36.58	36.60	36.62
1620	36.64	36.67	36.69	36.71	36.73	36.76	36.78	36.80	36.82	36.84
1630	36.87	36.89	36.91	36.93	36.98	36.98	37.00	37.02	37.05	37.07
1640	37.09	37.11	37.14	37.16	37.18	37.20	37.23	37.25	37.27	37.29
1650	37.31	37.34	37.36	37.38	37.40	37.43	37.45	37.47	37.49	37.52
1660	37.54	37.58	37.58	37.60	37.63	37.65	37.67	37.69	37.72	37.74
1670	37.76	37.78	37.81	37.83	37.85	37.87	37.89	37.92	37.94	37.96
1680	37.98	38.01	38.03	38.05	38.07	38.09	38.12	38.14	38.16	38.18
1690	38.20	38.23	38.25	38.27	38.29	38.32	38.34	38.36	38.38	38.40
1700	38.43	38.45	38.47	38.49	38.51	38.54	38.56	38.58	38.60	38.62
1710	38.65	38.67	38.69	38.71	38.73	38.76	38.78	38.80	38.82	38.84
1720	38.87	38.89	38.91	38.93	38.95	38.98	39.00	39.02	39.04	39.06
1730	39.09	39.11	39.13	39.15	39.17	39.20	39.22	39.24	39.26	39.28
1740	39.31	39.33	39.35	39.37	39.39	39.42	39.44	39.48	39.48	39.50
1750	39.53	39.55	39.57	39.59	39.61	39.64	39.66	39.68	39.70	39.72
1760	39.75	39.77	39.79	39.81	39.83	39.86	39.88	39.90	39.92	39.94
1770	39.96	39.99	40.01	40.03	40.05	40.07	40.10	40.12	40.14	40.16
1780	40.18	40.20	40.23	40.25	40.27	40.29	40.31	40.34	40.36	40.38
1790	40.40	40.42	40.44	40.47	40.49	40.51	40.53	40.55	40.58	40.60

CHROMEL vs. ALUMEL THERMOCOUPLE

Degrees Fahrenheit — Reference Junction 32° F.

°F	0	1	2	3	4	5	6	7	8	9
					Millivolts					
1800	40.62	40.64	40.66	40.68	40.71	40.73	40.75	40.77	40.79	40.82
1810	40.84	40.86	40.88	40.90	40.92	40.95	40.97	40.99	41.01	41.03
1820	41.05	41.08	41.10	41.12	41.14	41.16	41.18	41.21	41.23	41.25
1830	41.27	41.29	41.31	41.34	41.36	41.38	41.40	41.42	41.45	41.47
1840	41.49	41.51	41.53	41.55	41.57	41.60	41.62	41.64	41.68	41.68
1850	41.70	41.73	41.75	41.77	41.79	41.81	41.83	41.85	41.88	41.90
1860	41.92	41.94	41.96	41.99	42.01	42.03	42.05	42.07	42.09	42.11
1870	42.14	42.16	42.18	42.20	42.22	42.24	42.26	42.29	42.31	42.33
1880	42.35	42.37	42.39	42.42	42.41	42.46	42.48	42.50	42.52	42.55
1890	42.57	42.59	42.61	42.63	42.65	42.67	42.69	42.72	42.74	42.76
1900	42.78	42.80	42.82	42.84	42.87	42.89	42.91	42.93	42.95	42.97
1910	42.99	43.01	43.04	43.06	43.08	43.10	43.12	43.14	43.17	43.19
1920	43.21	43.23	43.25	43.27	43.29	43.31	43.34	43.36	43.38	43.40
1930	43.42	43.44	43.47	43.49	43.51	43.53	43.55	43.57	43.59	43.61
1940	43.63	43.66	43.68	43.70	43.72	43.74	43.76	43.78	43.81	43.83
1950	43.85	43.87	43.89	43.91	43.93	43.95	43.98	44.00	44.02	44.04
1960	44.06	44.08	44.10	44.13	44.15	44.17	44.19	44.21	44.23	44.25
1970	44.27	44.30	44.32	44.34	44.36	44.38	44.40	44.42	44.44	44.47
1980	44.49	44.51	44.53	44.55	44.57	44.59	44.61	44.63	44.66	44.68
1990	44.70	44.72	44.74	44.76	44.78	44.80	44.82	44.85	44.87	44.89
2000	44.91	44.93	44.95	44.97	44.99	45.01	45.03	45.06	45.08	45.10
2010	45.12	45.14	45.16	45.18	45.20	45.22	45.24	45.27	45.29	45.31
2020	45.33	45.35	45.37	45.39	45.41	45.43	45.45	45.48	45.50	45.52
2030	45.54	45.56	45.58	45.60	45.62	45.64	45.66	45.69	45.71	45.73
2040	45.75	45.77	45.79	45.81	45.83	45.85	45.87	45.90	45.92	45.94
2050	45.96	45.98	46.00	46.02	46.04	46.06	46.08	46.11	46.13	46.15
2060	46.17	46.19	46.21	46.23	46.25	46.27	46.29	46.31	46.33	46.36
2070	46.38	46.40	46.42	46.44	46.46	46.48	46.50	46.52	46.54	46.56
2080	46.58	46.60	46.63	46.65	46.67	46.69	46.71	46.73	46.75	46.77
2090	46.79	46.81	46.83	46.85	46.87	46.90	46.92	46.94	46.96	46.98
2100	47.00	47.02	47.04	47.06	47.08	47.10	47.12	47.14	47.17	47.19
2110	47.21	47.23	47.25	47.27	47.29	47.31	47.33	47.35	47.37	47.39
2120	47.41	47.43	47.45	47.47	47.49	47.52	47.54	47.56	47.58	47.60
2130	47.62	47.64	47.66	47.68	47.70	47.72	47.74	47.76	47.78	47.80
2140	47.82	47.84	47.86	47.89	47.91	47.93	47.95	47.97	47.99	48.01
2150	48.03	48.05	48.07	48.09	48.11	48.13	48.15	48.17	48.19	48.21
2160	48.23	48.25	48.27	48.29	48.32	48.34	48.36	48.38	48.40	48.42
2170	48.44	48.46	48.48	48.50	48.52	48.54	48.56	48.58	48.60	48.62
2180	48.64	48.66	48.68	48.70	48.72	48.74	48.76	48.79	48.81	48.83
2190	48.85	48.87	48.89	48.91	48.93	48.95	48.97	48.99	49.01	49.03
2200	49.05	49.07	49.09	49.11	49.13	49.15	49.17	49.19	49.21	49.23
2210	49.25	49.27	49.29	49.31	49.33	49.35	49.37	49.39	49.41	49.43
2220	49.45	49.47	49.49	49.51	49.53	49.55	49.57	49.59	49.61	49.63
2230	49.65	49.67	49.69	49.71	49.73	49.76	49.78	49.80	49.82	49.84
2240	49.86	49.88	49.90	49.92	49.94	49.96	49.98	50.00	50.02	50.04
2250	50.06	50.08	50.10	50.12	50.14	50.16	50.18	50.20	50.22	50.24
2260	50.26	50.28	50.30	50.32	50.34	50.36	50.38	50.40	50.42	50.44
2270	50.46	50.48	50.50	50.52	50.54	50.56	50.57	50.59	50.61	50.63
2280	50.65	50.67	50.69	50.71	50.73	50.75	50.77	50.79	50.81	50.83
2290	50.85	50.87	50.89	50.91	50.93	50.95	50.97	50.99	51.01	51.03
2300	51.05	51.07	51.09	51.11	51.13	51.15	51.17	51.19	51.21	51.23
2310	51.25	51.27	51.29	51.31	51.33	51.35	51.37	51.39	51.41	51.43
2320	51.45	51.47	51.48	51.50	51.52	51.54	51.56	51.58	51.60	51.62
2330	51.64	51.66	51.68	51.70	51.72	51.74	51.76	51.78	51.80	51.82
2340	51.84	51.86	51.88	51.90	51.92	51.94	51.96	51.98	52.00	52.01
2350	52.03	52.05	52.07	52.09	52.11	52.13	52.15	52.17	52.19	52.21
2360	52.23	52.25	52.27	52.29	52.31	52.33	52.35	52.37	52.39	52.41
2370	52.42	52.44	52.46	52.48	52.50	52.52	52.54	52.56	52.58	52.60
2380	52.62	52.64	52.66	52.68	52.70	52.72	52.74	52.76	52.77	52.79
2390	52.81	52.83	52.85	52.87	52.89	52.91	52.93	52.95	52.97	52.99

CHROMEL vs. ALUMEL THERMOCOUPLE

Degrees Fahrenheit — Reference Junction 32° F.

°F	0	1	2	3	4	5	6	7	8	9
					Millivolts					
2400	53.01	53.03	53.05	53.07	53.08	53.10	53.12	53.14	53.16	53.18
2410	53.20	53.22	53.24	53.26	53.28	53.30	53.32	53.34	53.35	53.37
2420	53.39	53.41	53.43	53.45	53.47	53.49	53.51	53.53	53.55	53.57
2430	53.59	53.60	53.62	53.64	53.66	53.68	53.70	53.72	53.74	53.76
2440	53.78	53.80	53.82	53.83	53.85	53.87	53.89	53.91	53.93	53.95
2450	53.97	53.99	54.01	54.03	54.04	54.06	54.08	54.10	54.12	54.14
2460	54.16	54.18	54.20	54.22	54.24	54.25	54.27	54.29	54.31	54.33
2470	54.35	54.37	54.39	54.41	54.43	54.44	54.46	54.48	54.50	54.52
2480	54.54	54.56	54.58	54.60	54.62	54.63	54.65	54.67	54.69	54.71
2490	54.73	54.75	54.77	54.79	54.81	54.82	54.84	54.86	54.88	54.90

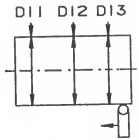

APPENDIX B
EXPERIMENT #3

RPM	START DIA.				END DIA.				CUTTING SPEED (SFM)	LENGTH OF CUT L	DISTANCE (INCH)	TEMPERATURE (deg. C)
	D11	D12	D13	Avg. D1	D21	D22	D23	Avg. D2				
116	7.598	7.594	7.590	7.594	7.596	7.593	7.588	7.592	230.6	10.0	-	93.3
146	7.596	7.593	7.588	7.592	7.590	7.589	7.572	7.584	290.2	10.0	-	127.2
224	7.590	7.589	7.572	7.584	7.590	7.588	7.568	7.582	444.7	10.0	-	139.4
290	7.590	7.588	7.568	7.582	7.588	7.586	7.565	7.580	575.6	10.0	-	377.8
360	7.588	7.586	7.565	7.580	7.584	7.582	7.649	7.572	714.4	10.0	-	544.4

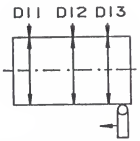

APPENDIX B (Contd.)
EXPERIMENT #4

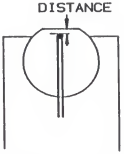

RPM	START DIA.				END DIA.				CUTTING SPEED (SFM)	LENGTH OF CUT L	DISTANCE (INCH)	TEMPERATURE (deg. C)
	D11	D12	D13	Avg. D1	D21	D22	D23	Avg. D2				
290	7.412	7.411	7.411	7.411	7.383	7.382	7.382	7.382	562.7	10.0	0.1360	376.7
290	7.383	7.382	7.382	7.382	7.379	7.369	7.340	7.362	560.5	10.0	0.1165	517.2
290	7.379	7.369	7.340	7.362	7.377	7.310	7.299	7.329	559.0	10.0	0.0775	616.7

Note: Distance of the thermocouple is measured before the start of each run.

Maximum temperatures were measured half way through each run. Average distance has therefore been considered for plotting.

APPENDIX B (Contd.)

EXPERIMENT #5

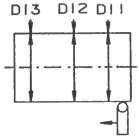

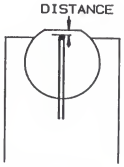

RPM	START DIA.			Avg.	END DIA.			Avg.	CUTTING SPEED (SFM)	LENGTH OF CUT L	DISTANCE (INCH)	TEMPERATURE (deg. C)
	D11	D12	D13	D1	D21	D22	D23	D2				
290	7.233	7.236	7.240	7.236	7.200	7.229	7.229	7.219	549.4	10.0	0.0561	155.0
290	7.200	7.229	7.229	7.219	7.169	7.170	7.177	7.172	548.1	10.0	0.0523	204.4
290	7.169	7.170	7.177	7.172	6.961	6.955	6.953	6.956	544.5	10.0	0.0304	593.0
290	6.961	6.955	6.953	6.956	6.925	6.910	6.890	6.908	528.1	10.0	0.0230	751.0

Note: Distance of the thermocouple is measured before the start of each run.

Maximum temperatures were measured half way through each run.

Average distance is therefore considered for plotting.

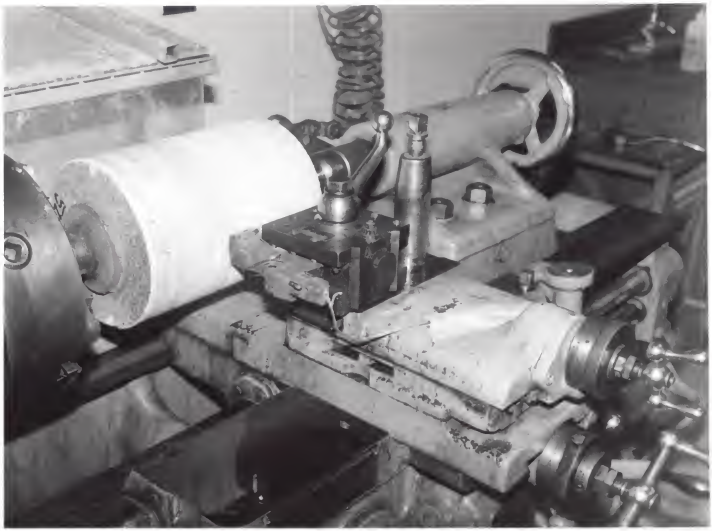

EXPERIMENTAL ARRANGEMENT

ACKNOWLEDGEMENTS

I wish to express my sincere appreciation and gratitude to Dr. Frederic C. Appl, Professor of Mechanical Engineering and Dr. Doris L. Grosh, Acting Head, Department of Industrial Engineering for their guidance and counsel throughout this work.

My appreciation and gratitude are also due to Mr. C. Carl Wilson, Associate Professor of Industrial Engineering for his valuable guidance, encouragement, and active participation throughout this project.

I am grateful to Dr. Gene L. Grosh, Associate Professor of Industrial Engineering for serving on my committee.

My thanks are also due to Mr. Francis B. Doll of the Department of Industrial Engineering for helping at every stage of the project and without whose effort, this project would not have been possible.

Finally my thanks are due to my family whose support and inspiration has helped me throughout my graduate study.

MEASUREMENT OF CUTTING TEMPERATURES IN SYNTHETIC DIAMOND CUTTERS DURING ROCK CUTTING

by

P. MADHUSUDHAN

B.S.(Honors), University of Madras, India, 1981

AN ABSTRACT OF A MASTER'S THESIS

submitted in partial fulfillment of the
requirements for the degree

MASTER OF SCIENCE

Department of Industrial Engineering

KANSAS STATE UNIVERSITY
MANHATTAN, KANSAS

1988

ABSTRACT

The introduction of synthetic polycrystalline diamond compact (PDC) cutters for use as cutters on oil well drill bits by General Electric in 1973 was a significant advancement in drilling technology. To realize the full potential of this type of cutter a theoretical model of cutting heat transfer and wear for these cutters was developed by Prakash. In order to obtain additional verification and refinement of the theoretical model, tool temperatures are experimentally measured using K type thermocouples. A study is done for using infrared radiation pyrometry for accuracy and flexibility in temperature measurement. The effect of cooling on tool wear is also studied. Experiment results confirm the theoretical model and reconfirm the theory regarding rapid diamond wear at the critical temperature. The results also suggest the existence of a strong possibility of film boiling of the coolant in actual downhole conditions resulting in localized dry rock drilling and rapid wear.